

# ASC DRD

**DRAFT Detector Alignment Sensing/  
Control Design Requirements Document  
LIGO-T952007-00-I; CDS to be added**

**David Shoemaker**

---

## 1 INTRODUCTION

This Design Requirements Document (DRD) addresses the requirements for the Detector Alignment Sensing/Control system. In addition, the conceptual designs, interfaces, and specifications are outlined. The system consists of several largely separable units, and both the effort and this document will maintain that division into the System Level requirements and overall design, the Initial Alignment, the Optical Lever, the Wavefront Sensing, and the Beam Centering.

This document will grow incrementally as the knowledge base is developed. The initial version will concentrate on the System Level requirements. At the present time (April 95), the sections on Initial Alignment, Wavefront Sensing, Optical levers, and Centering should be considered as informational only. The Control and Data System aspect (both local to the ASC and the interaction with the ‘CDS Backbone’) is yet to be integrated into this document.

The Design Requirements Document is organized so that all of the requirements on the alignment system (whether they impact the Initial Alignment, Optical Lever, the Wavefront Sensing, or the Centering) appear at the beginning of the System Level description. All of the material that follows is more or less influenced by the specific hardware and organization which is chosen to meet those requirements.

## 2 SYSTEM LEVEL ASC

### 2.1. Scope and Objectives

The overall ASC system acquires and maintains the angular and lateral alignment of the GW-sensing interferometer suspended optical components, and the angular and lateral positioning of the laser input beam. The first-time alignment of the interferometer and recovery of alignment after down-time are included. The IOO Mode Cleaner alignment and the beam pointing between the Mode Cleaner and the recycling mirror are also part of this task.

In the System Level ASC, the top-level requirements and subsystem division and coordination is determined. Detailed descriptions of the subsystems are given in sections below.

## 2.2. Performance Requirements for the overall ASC system

The performance which is required of the overall ASC system is called out here. It is summarized in Table 1, and described in more detail in the following paragraphs.

**Table 1: Performance requirements of the overall ASC system**

<i>Requirement</i>	<i>ASC Subsystem</i>	<i>Value</i>	<i>Paragraph</i>
allowed RMS misalignment per mirror, operation	Wavefront	$1 \times 10^{-8}$ rad	2.2.1., pg. 2
allowed RMS misalignment per mirror, acquisition	Initial	TBD; order of $1 \times 10^{-7}$ rad	2.2.2., pg. 3
allowed RMS de-centering per test mass DOF	Centering	3.5 mm	2.2.3., pg. 3
Time to achieve initial operational alignment	Initial	TBD; order of 24 hours	2.2.4.1, pg. 3
Time to achieve off-line to standby alignment	Initial	TBD; order of 1 hour	2.2.4.2, pg. 3
Time to achieve standby to on-line alignment	Initial	TBD; order of 10 sec	2.2.4.3, pg. 3
duration acquisition alignment is maintained	Optlev	TBD; order of 1 minute	2.2.5., pg. 4

### 2.2.1. Principal Interferometer optics angular alignment tolerance

The LIGO interferometers incorporate complex coupled optical cavities. In order to achieve optimal sensitivity, interferometer alignment with respect to the input beam must be maintained within a narrow range. An analytic model, based on a Gaussian mode decomposition, has been developed which can predict the sensitivity of complex systems of coupled optical cavities to misalignment. Results from this model have been verified experimentally. A strategy for detection and correction of misalignment based on this model has been developed. See Section 7.1. on page 35 for the approach to determining the requirement. The shot-noise limited signal-to-noise ratio for GWs is used as the measure of quality of alignment; misalignments lead to increased light on the antisymmetric (dark port) photo-detector as well as reduced coupling into the interferometer.

The calculation leads to a requirement of  $3 \times 10^{-8}$  radians rms alignment tolerance for each optic. Furthermore, a safety factor should be applied, TBD by the System Integration. We use a baseline safety factor of 3, leading to a requirement of  $1 \times 10^{-8}$  radians rms for each of the principal interferometer optics (four test masses, beamsplitter, and recycling mirror).

An additional consideration is the coupling of a static misalignment with input beam jitter. The sensitivity to this effect is TBD, but is estimated as follows.

The Max Planck group<sup>1</sup> analyzed a simple Michelson with equal arms, and found that there is an apparent phase

---

1. A Ruediger et al., Optica Acta 1981, vol 28 no 5 pg 641-658

change  $\delta\phi = \alpha k a(t)$  where  $\alpha$  is the angular misalignment,  $k$  the wavenumber for the laser light, and  $a(t)$  the translation beam jitter. This model for the interferometer is probably fairly accurate for the sidebands which circulate only in the ‘near’ interferometer (beamsplitter and near test masses). Given the LIGO requirement of about  $\delta\phi = 1 \times 10^{-8} \text{ rad}/\sqrt{\text{Hz}}$  and the angular alignment requirement of  $\theta \leq 1 \times 10^{-8}$  determined by the shot noise sensitivity, this leads to a translational beam jitter requirement of  $a(t) = 8 \times 10^{-10} \text{ m}/\sqrt{\text{Hz}}$ . For angular beam jitter, a simple model of an asymmetric interferometer (again, imagining the near-mirror Michelson with its asymmetry used in the Schnupp modulation scheme) leads to apparent length changes of  $\delta x = \Delta/\theta_0 \delta\theta$  for small motions  $\delta\theta$  around a static misalignment  $\theta_0$  and length asymmetry  $\Delta l$ . Using an asymmetry of 0.5 m, and the static misalignment matching the shot noise requirement, we have roughly  $\delta\theta = 2 \times 10^{-9} \text{ rad}/\sqrt{\text{Hz}}$ . The modal model will be applied to this problem to obtain a more realistic picture including the 4 km arm cavities.

### 2.2.2. Allowed RMS misalignment per mirror, acquisition

TBR. The interferometer must be sufficiently close to the correct alignment during the length control acquisition procedure that the set of error signals and the ‘plant’ (transfer functions from error signals to control signals) resemble those of the final ideally-aligned system. The signal-to-noise will be a secondary condition, but the system must have the majority of the power in the TEM<sub>00</sub> mode and the optical storage times must approximate the ideally-aligned case.

A first approximation to this requirement comes from an analysis of the sidebands which circulate exclusively in the recycling cavity. This highly-degenerate cavity shows a rapid displacement of the optic axis of the modulation sidebands with misalignment of the recycling mirror. Using the criterion that a shift of the optic axis by one beam-waist diameter is the maximum tolerable, the working value used is  $1 \times 10^{-7}$  rad. An improved estimate will be made requires the FFT model of the interferometer, because the assumption of negligible power in modes greater than the TEM<sub>00</sub>, TEM<sub>01</sub>, and TEM<sub>10</sub> is not maintained.

If necessary, the range of acquisition alignment could be increased by allowing misalignments of the recycling mirror as part of the acquisition strategy, causing a decoupling of the two arm cavities. An upper limit of alignment tolerance can be estimated by seeing what arm mirror misalignment would lead to marginal overlap of the incoming light and the cavity optical axis. This is roughly an angle of  $\theta \approx w_0/L = 2 \times 10^{-2}/4 \times 10^3 = 5 \times 10^{-6}$  rad.

### 2.2.3. Principal Interferometer optics centering tolerance

The performance specification is developed using a model for the coupling from a combination of offset from center and GW-band rotational motion to length changes. Note that the centering must be maintained within prescribed limits for both static positioning and dynamic ‘beam wander’ or optic motion. See Section 7.2. on page 36 for the approach to determining the requirement.

As excitation, we assume that the principal motion will be due to the uncorrelated forces due to the suspension coil driver output noise. This produces both translation and rotational excitation. For the additional noise due to the angular noise rest below that of the translation (GW-mimicking noise), the beam must be centered to within 0.3 of the mirror radius or 3.8 cm.

This leads to a requirement, assuming 8 uncorrelated degrees of freedom for the 4 test masses and a margin below the translational noise of 3 (in quadrature sum, a factor of 10), of 3.5 mm per mirror degree of freedom transverse to the main GW-sensing beam.

## 2.2.4. Transition times

These transition times, or maximum durations for major states of the ASC, will be determined from the specifications of the commissioning and operating scenario.

### 2.2.4.1 Time to achieve initial operational alignment

TBD. This is a procedure which is executed as part of the commissioning process, and happens quite infrequently: when a set of test masses is installed or a suspension is repaired, or when a new interferometer line is inaugurated. It will take of the order of one day, and is a largely manual procedure.

### 2.2.4.2 Time to achieve off-line to standby alignment

TBD. This procedure is executed when a change in the interferometer is made which does not seriously disturb the alignment; and example would be the pumpdown of an adjacent interferometer, or after the replacement of a laser. It will take of the order of one hour, and is a combination of automated and manual steps.

### 2.2.4.3 Time to achieve standby to on-line alignment

TBD. This procedure is executed each time the interferometer operating length is re-acquired. The duration will depend on the time since the interferometer was last locked, and may be almost instantaneous, the order of 1 second (if a check shows that the alignment is already suitable for acquisition), or may take the order of one minute if a new acquisition alignment must be made.

## 2.2.5. Duration over which acquisition alignment is maintained

TBD. This is the time over which an alignment is maintained which is close enough to the ideal (see Section 2.2.2.) to allow the length control system acquisition to take place, and without interference with the locking procedure. It will be of the order of 10 minutes.

## 2.3. Overall conceptual design

The ASC functions as a hierarchy, in ordering and in precision, of several subsystems. There are two kinds of Initial Alignment: The Bootstrap initial alignment covers the first installation of an interferometer. Its precision is sufficient to get beams down the 4 km tubes (angles of  $1 \times 10^{-5}$  rad) and is rarely performed; it is largely manual. The Recovery initial alignment takes place when a test mass is replaced or other disturbances cause a loss of Optical Lever control (and it follows any Bootstrap alignment); it will have a precision to place beams on mirrors over the 4 km baseline ( $2 \times 10^{-6}$  rad), and sets up Optical levers to their operational alignment.

The Optical Levers (resembling those on the circa 1994 40m prototype) have a low enough angular sensing noise in the GW band and a sufficient long-term stability ( $1 \times 10^{-8}$  rad) to allow operation of the interferometer for several minutes at a time for diagnostics and to bridge over short-term loss of lock in the longitudinal servo systems. The alignment maintained by the Optical lever is determined by manual or automated searches (possibly involving dithering or raster scanning).

The Wavefront System determines and maintains operational alignment under normal operating conditions. It cannot operate until the longitudinal servo system is in operation, but then continually updates the Optical lever system (which remains in operation) with the ideal alignment (as determined by measures of the interferometer itself).

The Centering System keeps the beams centered on the mirrors to avoid transfer of rotational mirror motion to longitudinal (GW, gravitational wave) signals.

The actuators to effect the alignment are the SUS Suspension actuators, the (subsystem TDB) Seismic stack support positioners, and the IOO beam pointing mirrors. There is a close interaction with the design and function of the LSC Length control system.

### 2.3.1. States

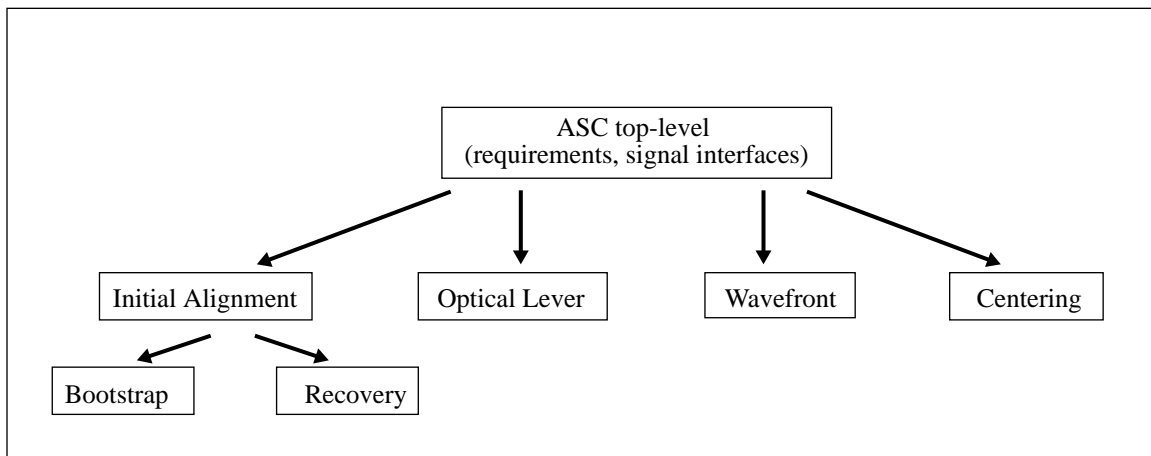


**Figure 1: Requirements flowdown for the ASC system**

See Figure 2 on page 6 for a top-level summary of the states (ovals), processes (rectangles), and some decision points (diamonds) for the ASC.

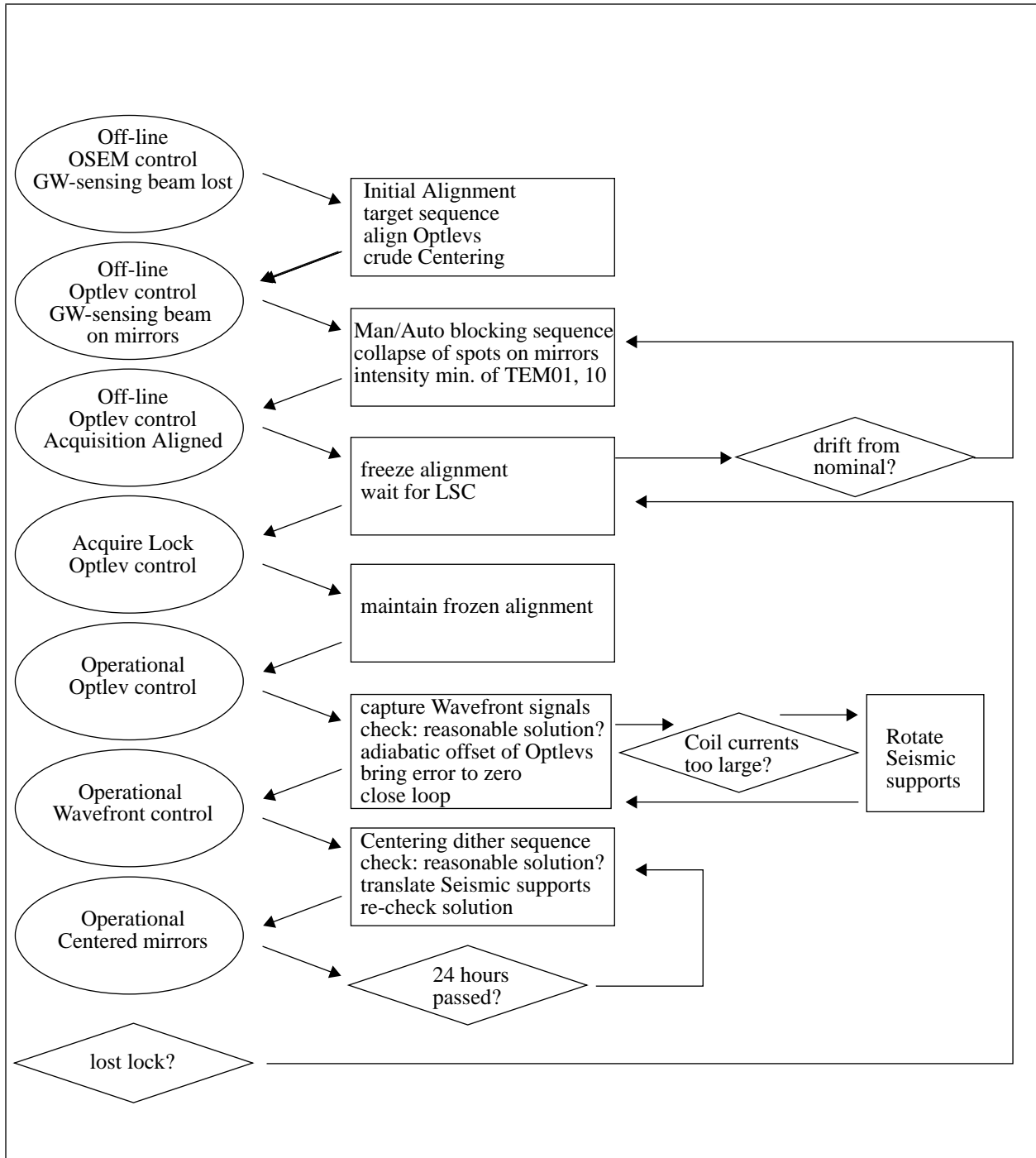


Figure 2: States and processes of the ASC

## 2.4. Interface Requirements

### 2.4.1. Parameter interfaces: inputs to the ASC System design

These parameter interfaces which put constraints on the ASC System design are summarized in Table 2 on page 7, and are discussed in the paragraphs below. These parameter interfaces are relevant for all of the ASC subsystems (Ini-

tial alignment, Optical lever, Wavefront, Centering).

**Table 2: Interface Parameters for the top-level ASC**

<i>Requirement</i>	<i>Source</i>	<i>Value</i>	<i>Paragraph</i>
gravitational wave sensitivity, shot noise region	Sys Int	$x_0 = 1 \times 10^{-19} \text{ m}/\sqrt{\text{Hz}}$ $f_{\text{knee}} = 90 \text{ Hz}$	2.4.1.1
allowed degradation in GW sensitivity, shot noise region	Sys Int	$D=0.9$ ; $x' = x_0/D$ TBR	2.4.1.1
horiz. seismic motion of test mass, operational	SUS	TBD; e.g., DHS RMS motion doc.	2.4.1.2
horiz. thermal motion of test mass, operational	SUS	TBD; e.g., SUS DRR	2.4.1.2
allowed sensitivity degradation in seismic region	SYS	$f_{\text{cutoff}}^{\text{degraded}} = 1.01 f_{\text{cutoff}}$ TBR	2.4.1.2
allowed sensitivity degradation in thermal region	SYS	$D=0.9$ ; $x' = x_0/D$ TBR	2.4.1.2
length sensing rms deviation from dark fringe	LSC	TBD, order of $10^{-5}$ rad	2.4.1.3
alignment requirement for acquisition of LSC	LSC	TBD, order of $1 \times 10^{-7}$ rad	2.4.1.4
alignment requirement for stability of LSC	LSC	TBD, order of $10^{-7}$ rad	2.4.1.4
curvature mismatch of arms	COC	$0.05 \lambda$ for each mirror	2.4.1.5
power scattered out of $\text{TEM}_{00}$ but on mirrors	COC	20 ppm	2.4.1.5
alignment req. for Mode Cleaner	IOO	TBD	2.4.1.6
beam jitter at input to recycling mirror	IOO	TBD	2.4.1.7
transverse seismic motion, operational	SUS	TBD; e.g., DHS RMS motion doc.	2.4.1.8
horiz. seismic motion of test mass, standby	SUS	TBD; e.g., spero/dhs scenario memo	2.4.1.8
tilt seismic motion of test mass, operational	SUS	TBD; e.g., DHS RMS motion doc.	2.4.1.9
tilt thermal motion of test mass, operational	SUS	TBD; spectrum	2.4.1.9
twist seismic motion of test mass, operational	SUS	TBD; e.g., DHS RMS motion doc.	2.4.1.9
twist thermal motion of test mass, operational	SUS	TBD; spectrum	2.4.1.9
distortion of support slab, non-operational	FAC	TBD; spectrum	2.4.1.10
support slab distortions during operation	FAC	TBD	2.4.1.11

<i>Requirement</i>	<i>Source</i>	<i>Value</i>	<i>Paragraph</i>
tilts of center to end slab	SYS	TBD (order of $10^{-7}$ )	2.4.1.12
operations: recovery time after pumpdown	SYS	TBD (order of 10 min)	2.4.1.13
operations: recovery time after lift tank oper.	SYS	TBD (order of 10 min)	2.4.1.13
operations: recovery time after dropout	SYS	TBD (order of 10 sec)	2.4.1.13
operations: design continuous locking time	SYS	TBD (order of 24 hours)	2.4.1.13

### 2.4.1.1 SYS: shot-noise limited gravitational wave sensitivity

The degradation of the contrast and the coupling into the interferometer determine the static angular alignment requirement.

- sensitivity in shot-noise limited region; allowed degradation due to misalignment. This is written as  $x_{\text{nominal}} = x_0 \sqrt{1 + (f/f_{\text{knee}})^2}$  with prescribed  $x_0 = 1 \times 10^{-19} \text{ m}/\sqrt{\text{Hz}}$  and  $f_{\text{knee}} = 90 \text{ Hz}$
- allowed degradation  $D_{\text{shot}}$  in shot noise defined by a compromised position sensitivity  $x' = x_0/D_{\text{shot}}$  with an assumption of a negligible change in the knee frequency. The assumption is that the noise sources which will cause the degradation add in quadrature to the existing noise. The coefficient could also be described in this light.

### 2.4.1.2 SYS: seismic and thermal noise limited gravitational-wave sensitivity

We require that the noise in this region not be seriously increased by the misalignment in angle or centering. We assume that the various sources of noise add in quadrature (square root of sums of squares).

- interferometer sensitivity in seismic and thermal noise limited spectral region. For the Seismic noise, the seismic noise contribution is assumed to fall as a high power of frequency,  $x_{\text{seismic}} = K \left( f - f_0^{\text{stack}} \right)^{2n}$ , with  $n \approx 12$  where  $K$  is a constant,  $f_0$  is the stack frequency at which rapid rolloff starts, and  $n$  is related to the ground noise spectrum, number of layers in the stack and its internal damping, and the pendulum suspension. The seismic noise is characterized by a cutoff frequency  $f_{\text{seismic cutoff}}$ , defined by a frequency at which the overall interferometer sensitivity is 10 times  $x_0$ , the shot noise at frequencies well below the knee frequency  $f_{\text{knee}}$  for the arm cavities. For the baseline seismic stack and shot noise, this gives TBR  $f_{\text{seismic cutoff}} = 40 \text{ Hz}$ .
- allowed degradation in sensitivity due to miscentering in seismic noise limited region. This is expressed as a degradation (i.e., increase) in cutoff frequency  $f_{\text{seismic cutoff}}' = f_{\text{seismic cutoff}} D_{\text{seismic}}$  (frequency at which e.g., the sensitivity is 10 times shot noise) in the seismic noise regime. This approach better describes the character of the compromise than would an increase in the noise level at a given frequency.
- For the Thermal noise, we assume that the primary noise is due to the pendulum mode thermal excitation, and write

$$x_{\text{th}} = x_{\text{th}}^{100 \text{ Hz}} \left( \frac{100 \text{ Hz} - f_{\text{pend}}}{f - f_{\text{pend}}} \right)^{\frac{3}{2}} \quad (\text{EQ 1})$$

- allowed degradation in sensitivity in thermal noise limited region due to miscentering. This is written as a degradation  $D_{\text{thermal}}$  in sensitivity for frequencies in the thermal noise regime:  $x'_{\text{th}} = (x_{\text{th}}/D_{\text{thermal}})$ .



### 2.4.1.3 LSC: length sensing configuration and performance

The configuration of the length sensing system determines much of the configuration of the Wavefront Sensing system, as the same modulation frequencies are used, and possibly the same pick-off positions. The deviations from a perfect lock influence the Wavefront Sensing error signal. The parameters to be given are:

- optical design (lengths, radii, transmissions, pick-off positions)
- modulation frequencies
- relative intensities and modulation depths of the carriers and sidebands
- anticipated deviations from zero error signal at each of the output ports

These requirements are used in the detailed design of the Wavefront sensing system, and the requirements directly below.

### 2.4.1.4 LSC: length control alignment requirements

Both of these requirements will follow the establishment of a detailed Optical Sensing model (placement of pick-offs, choice of frequencies, etc.). These influence the specifications for the Optical Lever performance before lock but during acquisition. The parameters to be given are:

- alignment requirements for acquisition of length control
- alignment requirements for stability/conditioning of length servo system

### 2.4.1.5 COC: core optics requirements

These requirements influence the quality of the error signal recovered by the Wavefront Sensing. The parameters to be given are:

- allowed curvature errors in the interferometer optics
- allowed medium-scale roughness on the interferometer optics (net effect of surface and coating)

### 2.4.1.6 IOO: mode cleaner requirements

The Mode Cleaner Optical Lever and (possibly) Wavefront Sensing system needs this information (may be generated in LSC or ASC, TBD). The parameters to be given are:

- requirements for alignment and pointing for correct MC operation
- requirements for alignment and pointing for correct interferometer operation
- angular noise requirements to keep jitter below the ambient leaving the MC

### 2.4.1.7 IOO: beam jitter at input to recycling mirror

The beam jitter at the input to the interferometer can couple with a static misalignment or asymmetry (accidental or intentional) to produce an apparent path length change. This noise mechanism has been only crudely modeled to date, but may put very severe constraints on the beam jitter in angle and position even for perfect optics. For perfect optics, the modal model can deliver the required information; for the case of imperfect optics, the FFT model will be required. The parameters to be given are:

- the translational beam jitter in the GW band
- the angular beam jitter in the GW band

### 2.4.1.8 SEI: transverse translational seismic motion of the suspended masses

This information about horizontal or vertical transverse motion is used to calculate RMS (including very slow drift) deviations from ideal centering, and is one of the inputs to the centering requirement calculation. The information

should take the form of a spectrum or equivalent. In particular, if the test mass angular motion is increased above the seismic level by the controller, this changes the centering requirement. This information will be needed operating/non-operating conditions:

- normal operation
- pumpdown, lift tank operations, crane operations

#### **2.4.1.9 SEI: rotational seismic and thermal motion of the suspended masses**

This is one of the inputs to the centering requirement calculation. The information should take the form of a spectrum or equivalent. In particular, if the test mass angular motion is increased above the seismic level by the controller, this changes the centering requirement. This information will be needed operating/non-operating conditions (the latter to know the range required of the sensing system to recover centering after a significant change):

- normal operation
- pumpdown, lift tank operations, crane operations

#### **2.4.1.10 FAC: distortions of the support slab (within one station), non-operational**

This determines the required range of the Optical Lever during standby (non-operation), e.g., during pumpdown, lift tank operations, crane operations. Distortions during normal operation will be arrived at by discussion between Facilities and ASC.

#### **2.4.1.11 FAC: distortions of the support slab (within one station), operational**

This determines the length of time the Optical Lever can maintain operational, or acquisition, pointing precision. The optical lever is required at least to act as a bootstrap into operation. This means that the optical lever system, however it is constructed, must be able to maintain a pre-determined angle with a precision of the capture range of the length control and wavefront sensor system between a manual setting of the mirror angles and the end of the lock sequence. The capture angle is TBD (see section 2.2.2., pg. 3), as is the duration associated with lock acquisition (see section 2.2.5., pg. 4). However, we estimate that the required acquisition angle is roughly  $1 \times 10^{-7}$  radians, and the time is roughly 10 minutes.

If the optical lever is as we have built them to date with a roughly 50m long arm, then this turns into a requirement that the top of two monuments separated by the beam tube manifold diameter (roughly 2 m) at the mid-height of the beam tube (roughly 1.5 m from the slab top) must not move by more than roughly  $1 \times 10^{-7}$  m over 10 minutes; this corresponds to changes in the slab top angle between the two monument bases (separated by 2 m) of  $7 \times 10^{-8}$  radians. Alternative geometries for the optical lever may soften this requirement (either by bringing the laser and return beam closer together or by decoupling the possibly common support for the laser and photodiode from the slab). Other alternatives are discussed in the Appendix Section 8.3.1. on page 37 and following sections.

##### **2.4.1.11.1 Modeling of likely slab foundation distortions**

A study of a foundation concept for the LIGO corner and end stations has been performed. The objective of the study (for the ASC) was to quantify the temporal stability of the foundation concept and determine its suitability for supporting the operation of an Optlev alignment system. The minimal operational requirement of the Optlev, as previously stated, is that of being capable of initial lock acquisition of the fabry-perot cavities (requiring stability of order  $1 \times 10^{-7}$  rad for tens of minutes) whereas the maximal requirement of the Optlev is that of being capable of long-term alignment of the operating LIGO (requiring stability of order  $1 \times 10^{-8}$  rad for tens of minutes to hours).

The foundation concept studied was that of a 50 m by 50 m by 1m monolithic mat, composed of reinforced concrete, resting on soil characteristic of the Hanford, WA site. Structural, thermal, and tidal loadings were applied to finite ele-

ment models of the foundation and the temporal responses of each was considered. Many iterations of loadings and boundary conditions availed foundation performance information indicating that the concept is capable of supporting the Optlev in achieving its primary alignment objective of fabry-perot lock acquisition. The concept should not, however, be considered useful for maintaining Optlev stability suitable for long-term alignment of the operating LIGO even though it is capable of this level of stability for the order of a few minutes. These conclusions are valid when the following criteria are satisfied:

- The foundation's edges are structurally isolated from their surroundings.
- The foundation's edges are thermally isolated from their surroundings.
- The foundation's sole vibrational excitation is that of the standard LIGO input power spectrum applied only at the foundation's lower surface.
- The foundation's upper surface is continuously exposed to air maintained near room temperature.

#### 2.4.1.12 SYS: tilts and displacements of the center slab with respect to each end/mid slab

This determines the possible use of the Optical Lever during operation; while measures can be taken local to a given slab to improve the stability, the slabs move with respect to each other as determined by tidal and meteorological forces. The most significant inputs are the microseismic peak (around 0.13 Hz, or 7 sec period) and tidal motions (many frequencies, but most important at periods of 6 and 12 hours).

##### 2.4.1.12.1 Microseismic motion

The microseismic peak is measured<sup>1</sup> to lead to tilts of  $1 \times 10^{-7}$  rad pk-pk for an isolated monument, taking place over periods of 6-8 seconds. This value varies with geographical location, and seismic and meteorological activity. The accepted model<sup>2</sup> is that these are surface waves, travelling at 3-4 km/sec. The sources are somewhat localized, but there are many sources from unpredictable directions. if the velocity is 3.5 km/sec<sup>3</sup>, frequency 0.15 Hz, then the wavelength of the wave is roughly 23 km, and the 4 km length of the LIGO arms puts us at 1/5 wavelength of the seismic motion; this leads to relative peak-to-peak tilts for one arm of about  $4 \times 10^{-8}$  rad, with each arm effectively independent.

##### 2.4.1.12.2 Tidal motions

Typical measured amplitudes of surface angles due to tides (direct, not compensated for the ocean) are  $1 \times 10^{-7}$  rad pk-pk<sup>4</sup>. Greater tilts are observed when the ground is quite dry<sup>5</sup>, leading to daily pk-pk variations as great as  $3 \times 10^{-7}$ . Measurements in a mountainside accelerator tunnel show tidal tilts of  $4 \times 10^{-7}$  rad pk-pk<sup>6</sup>. These variations can take place over 6 hours, leading to a change in alignment of a slab by  $1 \times 10^{-8}$  rad in 2 hours. These values are not relative; for a simple earth model, the difference between tilts at the center and end slabs is the relevant value, but larger motions due to small-scale irregularities of the underlying earth structure are seen, and it seems prudent to carry the full value.

- 
1. Wyatt et al., J Geophys Res., Vol 93, No B8, pg 9197 (1988); graph labeled 7803E325-7 supplied by R. Weiss to dhs, 'Vault in Harvard, Mass' (from Draper?)
  2. Duncan Agnew (619 532 2590); Charles Bob Hutt (505 846 5646); Alan Rohay
  3. Agnew, Rev Geophys, Vol 24, No 3, Pg 579 (1986)
  4. Wyatt et al., Geophys. Res. Lett., Vol 9, No 7, pg 743 (1982)
  5. Wyatt et al., J Geophys Res., Vol 93, No B8, pg 9197 (1988)
  6. Tekeda et al., KEK Preprint 93-61 (1993)

### 2.4.1.12.3 Meteorological effects

There are significant changes in height due to passing weather patterns due to the change in atmospheric pressure. Values for several sites<sup>1</sup> give 0.5 to 1mm per 1 mbar pressure change, and storms bring changes of 20 to 40 mbar over a 24 hr period with resulting height changes of 20 mm pk-pk (with a frequency of about 1/month in Boulder, CO or Onsala, Sweden; do not know for LIGO sites). Storms are roughly gaussian in pressure profile and can reach 1000 km in width; we take a velocity of 200 km/hr, so might expect a storm to pass in 5 hrs. An estimate of the resulting largest height difference between center and end stations is 1 mm, or an angle change of  $2.5 \times 10^{-7}$  rad over 5 hours.

### 2.4.1.13 SYS: operations scenario

This refers to the time scales for the alignment systems to function after perturbations due to commissioning and/or 'normal' loss of lock. A natural set of parameters from the ASC standpoint would be as follows, but the form of the information should be determined by SYS.

- time to recover alignment after pumpdown
- time to recover alignment after lift tank operation
- time to relock longitudinal servo and time to regain operation after short dropout
- design continuous locked time

## 2.4.2. Parameter interfaces: demands made by the ASC System

These are requirements that the ASC system imposes on its interfaces with the rest of the detector and on the facilities. A summary is found in Table 3 on page 12.

**Table 3: Requirement demands placed by the ASC on other systems**

<i>Requirement</i>	<i>Target</i>	<i>Value</i>	<i>Paragraph</i>
suspended-mass actuator angular range	SUS	TBD; order of $3 \times 10^{-4}$ rad	2.4.2.1
suspended-mass actuator system angular noise	SUS	TBD; order of 1/3 natural seismic angular noise	2.4.2.2
stack translation/rotation actuator resolution	SEI	order of 20 $\mu$ m	2.4.2.3
stack translation/rotation actuator range	SEI	TBD; order of 3 cm	2.4.2.3
stack translation/rotation actuator acceleration spectrum	SEI	TBD; order of LIGO seismic acceleration	2.4.2.3

### 2.4.2.1 SUS: suspended-mass actuator angular range

The largest demand on the suspended-mass angular actuator will be made during initial alignment, when scans through angle will be made for searches of the beam tube aperture. Using GPS and a baseline of 50m, an initial angle of  $5\text{mm}/50\text{m} = 1 \times 10^{-4}$  rad can be established, and so this (with a safety factor) sets our need for this actuator in attitude. In altitude, the actuator must have a means to bring the possibly imperfectly balanced mirror to the nominal angle, and then the same range as the attitude must be available from that point. Note that this parameter interacts with Section 2.4.2.3 below.

### 2.4.2.2 SUS: suspension's actuator noise, direct and indirect

The actuators on the suspended masses must not produce angular motion at a level that adds significantly to the fil-

1. Van Dam et al., J Geophys Res., Vol 93, No B2, pg 1281 (1987)

tered seismic noise. This may turn out to be a point for trade-off: If there are significant technical difficulties in meeting this requirement, and the centering requirement could be made more stringent instead.

- angular noise motion of the suspended masses due to noise in driver electronics to be less than TBD; order of ( $<1/3$  in linear measure,  $1/10$  in quadrature sum) that of natural seismic noise
- other couplings due to miscentering/misalignment of suspension's actuators with respect to magnets, also dynamic effects, to be less than ( $<1/3$ ) seismic coupling. In particular, note the fact that the  $dF/dx$  curve is much narrower perpendicular to the normal suspension's actuator axis.
- actuators on suspended masses: bandwidth, noise to be sufficient (ASC should not drive this requirement)

### 2.4.2.3 SEI: seismic stack translation/rotation actuators

The ASC will use these actuators during operation to maintain the suspension's actuator coil currents to a minimum and to permit translations of the suspended mass in the vertical direction. The following parameters will be required:

- resolution: the actuators must have a smallest motion which allow rotations around the vertical axis (attitude, twist, or yaw) of the entire stack which are smaller (by a safety margin of 10) than the largest attitudinal angular motion which can be achieved using the suspension's actuators (Section 2.4.2.1). This leads to a requirement of  $3 \times 10^{-5}$  rad for the stack support actuators, or about 60 microns over a 2m stack baseline. Similarly, the translational resolution must meet the requirements for centering of the beams on the test masses. This is, with a safety factor of 10, TBD of the order of 1 mm for vertical and horizontal motion.
- range: The total range should be sufficient to allow significant motions away from the ideal centered point to accommodate long-term stack drift, and diagnostics involving de-centering of the beam; this is  $\pm 3$  cm. However, the  $60 \mu\text{m}$  resolution needed for daily compensation of the translations and rotations of one stack with respect to the others (on the same slab, on the remote slabs) need only be achievable over a range of TBD the order of  $500 \mu\text{m}$  (determined by facility distortions in excess of natural seismic motions).
- noise: any noise generated during motion must be comparable to the ambient ground motion (within the excess allowed by SysInt).
- acceleration: because these actuators must perform while the interferometer is operational and the accelerations must not exceed the limits on excess vibration defined by SysInt for the facility.

### 2.4.3. Physical interfaces

The detailed physical interfaces for the various subsystems of the ASC are described in the sections below which deal with the subsystems structures (e.g., 3.2). The System Level ASC has no physical interfaces; it is an organizational structure for the physical subsystems.

### 2.4.4. Coordination and divisions between ASC subsystems

The interfaces between the subsystems of the ASC are given in detail in the subsections dealing with the subsystems. Here is an overview of those interfaces. We describe the baseline configuration (traditional Optlev, expected slab stability).

#### 2.4.4.1 Block diagrams of system: hierarchy of subsystems

See Figure 3, "ASC Sequences and principal signal paths," on page 14. In this Figure, the principal signal flow into the ASC is indicated on the left side; the components of the ASC are in the middle, showing the downward flowing sequence of steps, and the focus of input of information to the Optical Lever; the signal flow from the ASC to external subsystems is shown at the right.

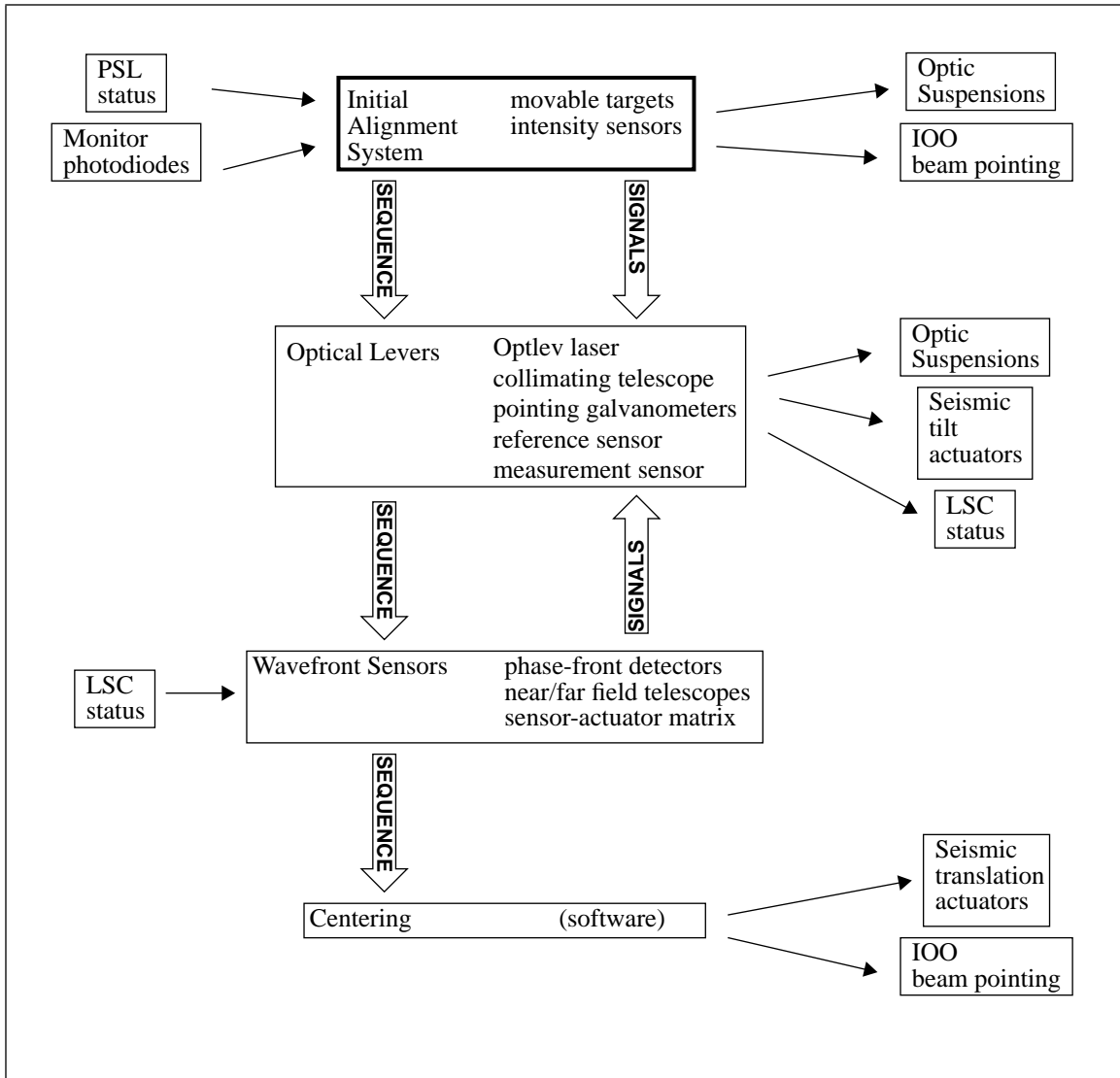


**Figure 3: ASC Sequences and principal signal paths**

## 2.4.4.2 Control bandwidth and dynamic range, baseline configuration

### 2.4.4.2.1 Initial alignment

2.4.4.2.1.1 Bootstrap: Manual procedure; hours in duration; use of Bulls'-eyes and GPS monuments.

2.4.4.2.1.2 Recovery: A manual or automated scan of a small range of alignments is made to bring the instrument to the point where acquisition is possible. This may be a simple raster scan with repeated attempts at closing the length control servo system (this resembles the circa-1994 prototype (FMI, 40m) approach), or a more sophisticated solution using the spot pattern in the cavities (monitored on a beam from the wedged surfaces of the optics). This process will take on the order of TBD 10 minutes.

### 2.4.4.2.2 Optical lever

2.4.4.2.2.1 Recovery: The Optical Lever holds a determined alignment with a long-term stability (of roughly

10 minutes or longer) sufficient to allow length acquisition, so that a manual or automated search for an acceptable acquisition alignment can be made. The angular orientation of the masses is held in a servo with sufficient gain-bandwidth to maintain control of the angle (against seismic noise), with offsets to the Optlev servo summing junction from the Initial Alignment Recovery system to guide the mirror through the scan (see 2.4.4.2.1.2, pg. 13). The pointing noise need not be low enough to allow operational GW sensitivity (i.e., smaller series resistors in the suspension actuators can be acceptable).

2.4.4.2.2.2 Operation: The Optical Lever holds a determined alignment with a medium-term stability (of roughly 1 minute or longer) sufficient to allow operation. The angular orientation of the masses is held in a servo with sufficient gain-bandwidth to maintain control of the angle (against seismic noise), with offsets to the Optlev servo summing junction from the Wavefront system (see 2.4.4.2.3, pg. 15) to maintain operational alignment. The pointing noise must be low enough to allow operational GW sensitivity, given centering tolerances or other feedthrough from intended angular control signals to length/GW signals. The control system must be designed to ensure that no significant coupling takes place from the (corrupted) long-term optical lever signals to suspension actuators.

### 2.4.4.2.3 Wavefront sensor

The wavefront sensor plays no role in the alignment system until the length control system is locked. At that point, the wavefront sensor signals are applied to the Optlev servo summing junctions to update the pointing. The update occurs at frequencies significantly lower than the mechanical resonances of the suspension (below roughly 0.3 Hz) and significantly lower than the inverse optical storage times (approximately 3 Hz) to ensure independence of the length and alignment servo systems. When the interferometer loses length lock, the offsets from the Wavefront sensor are held at their last operational value so that the interferometer remains nominally aligned for a quick Recovery cycle. The hardware will be designed to allow an alternative configuration where the wavefront sensor is used in place of the Optical lever, with the state change involving a complete switch from the Optlev sensor to the Wavefront sensor.

### 2.4.4.2.4 Centering

The baseline assumption is that the facility and seismic-suspension system is sufficiently stable that only rare (less frequently than daily), periodic, updates to the centering will be needed. The process of determining the correct centering by dithering angles, moving, re-dithering each test mass will require of the order of 1 minute and will probably degrade the GW sensitivity for that period of time but will not cause the interferometer to lose lock.

## 2.5. Physical and Environmental requirements

The physical requirements are given in the individual subsystem sections below.

## 2.6. Test plan

Most of the parts of the overall ASC can be tested separately, and these test plans are described in the individual subsystem sections below. Exceptions are in the overall coordination (state switching) and the nested servoloop that links the Optical lever ('high bandwidth', approx. 3 Hz Unity Gain Frequency) and the Wavefront sensor ('low bandwidth', approx. 0.1 UGF). In addition, the systems use the Suspension and Seismic stack support actuators, and the coordination with these must be tested or modeled to satisfaction.

The design philosophy is to separate the Optlev and Wavefront servoloops in bandwidth to make them virtually decoupled. The servoloops do not require extremes of bandwidth or delicate design trade-offs. The wavefront sensor will operate in a control system with time constants considerably longer than those of the optical storage time in the

interferometer and longer than the mechanical resonance (pendulum suspension) periods. Thus, a non-realtime steady-state emulation of the interferometer should be sufficient to test the cross-coupling in the linear control systems and the state switching. The modal model is to be used to predict the interferometer response to a misalignment (or length error). The Suspension and Seismic subsystems will require a model; perhaps supplied by those subsystems.

Aspects of the ASC which will be tested in such an emulation:

- The response of the locked interferometer to a misalignment
- sensitivity of the system to accidental cross-coupling in the sensor-actuator matrix
- length-alignment coupling in the steady state
- state changing based on sensor inputs; prioritizations, illegal states
- to be continued

Aspects which will not be tested in this emulation:

- control system dynamic characteristics (assumed trivial)
- dynamic cross-coupling of any kind
- problems due to high-order spatial modes (greater than  $TEM_{01}$ ,  $TEM_{10}$ ,  $TEM_{20}$ )
- depending on the model, electronic saturation/mismatch/nonlinearity, noise

## 3 INITIAL ALIGNMENT SUBSYSTEM

### 3.1. Scope and Objectives

The Initial alignment system has two functions:

- To carry out the first alignment of a given interferometer, and
- to recover alignment after pumpdown, lift operation, repair, etc.

The detailed design of the Initial Alignment system is scheduled for FY 96. Some initial considerations are needed to ensure that the Facilities and Vacuum Equipment interfaces are generated in a timely fashion; the cursory description below is only designed to fulfill that need.

### 3.2. Functional and Performance specifications

TBD.

### 3.3. Conceptual Design

A sequence of steps is followed which uses precision monuments to bring the interferometer into acquisition alignment. The present rough conceptual design is the following:

Movable targets are to be mounted in the vacuum equipment at points as far as practical from the masses (near the  $LN_2$  pumps, similar at mid and end stations). Their position will be linked to monuments outside of the vacuum system which are fiducials for the Initial alignment; their inertial position must be determined to within 2 mm to allow sufficient precision to determine the pointing of the beam. The targets resemble iris diaphragms, except that the center point can be adjusted to agree with the centers of beams for the various interferometers (full and mid-length). Sensors



are mounted on the iris diaphragms to allow detection of the position of an assumed gaussian beam on the diaphragm. The diaphragms can block the beam to aid in locking and diagnostics.

### 3.3.1. Bootstrap Alignment

The following is a rough sequence of events for the first steps of the initial alignment:

- Bring masses under Suspension sensor-actuator control
- GW-sensing beam to near target in straight-through arm
- Autocollimate recycling mirror crudely
- Misalign recycling mirror to avoid accidental multiple beam round trips
- Autocollimate near mirror crudely
- Misalign near mirror to avoid accidental multiple beam round trips
- GW-sensing beam to far target (raster or spiral scan if needed)
- GW-sensing beam on far mirror
- GW-sensing beam returned to near target (far mirror angle)
- Optical levers initial rough alignment
- Rough centering of beams on mirrors
- Repeat for 90° arm

### 3.3.2. Recovery/Acquisition Alignment

The sequence continues as below; in the case of a minor configuration change, or loss of lock, the sequence is entered at the appropriate point:

- center Optical levers in range
- Maximize  $TEM_{00}$  ( $TEM_{01} < TBD$  approx 10%) in straight-through arm (freely swinging or driven, not locked)
- Block arms
- Maximize Michelson contrast
- lock Michelson (dither possible if needed)
- optimize recycling mirror angle  $TEM_{00}$  ( $TEM_{01} < TBD$  approx 10%) in recycling cavity
- Store Recycling mirror alignment, misalign
- Unblock arms
- Maximize  $TEM_{00}$  ( $TEM_{01} < TBD$  approx 10%) in 90° arm (freely swinging or driven, not locked)
- Realign recycling mirror

The system is most easily described as a sequence. The masses are assumed at the outset to be under active damping control by Suspension sensor/actuators control systems (resembling 1994 OSEMs in function).

The initial Bootstrap alignment covers the first time effort to get a GW-sensing beam down the 4km beam tube. This involves relating the GW-sensing beam position in the center station to precision monuments, getting the GW-sensing beam down the beam tube onto the far mirror and centering detector. Some manual iteration of angles follows to get beams falling on mirror surfaces. To avoid preliminary (confusing) multiple reflections, first the near mirror is intentionally misaligned and the beam roughly centered on the far mirror of the straight-through path; then the back mirror angle is adjusted to bring the spot back onto the (misaligned) near mirror. Optical levers with lever arms of roughly 50m are set up on each of the interferometer optics, using monuments whose position is known to GPS accuracy (<5 mm).

The Recovery alignment takes the system to the alignment required for acquisition of the length control servo. The

Optlevs are centered in their range. Isolated arm cavity intensity patterns (from wedge beams) and the simple blocked arm (or misaligned back-mirror) Michelson are examined using CCD cameras, image analysis, and closed loop feedback to maximize the power the TEM<sub>00</sub> mode or maximize the contrast.

## **3.4. Interface Requirements**

### **3.4.1. Parameter Interfaces: inputs to the Initial Alignment design**

#### **3.4.1.1 Centering**

signals from centering detector on far mirrors

### **3.4.2. Parameter Interfaces: demands made by the Initial Alignment design**

#### **3.4.2.1 IOO**

Pointing commands for the GW-sensing beam

Matching (gaussian parameter) instructions (until the system is resonant, the matching is not predetermined but must be within close control to get down 4km tube)

#### **3.4.2.2 COC**

commands to align/misalign/scan via suspension

#### **3.4.2.3 Optlev**

commands to align (manual or automatic, TBD) the Optlevs once within range

summing point offsets to Optlevs for precision scanning and pre-alignment

#### **3.4.2.4 Wavefront**

no interface

#### **3.4.2.5 Centering**

signals from centering detector on far mirrors

commands to centering for fine beam placement on far mirrors

#### **3.4.2.6 LSC**

command to indicate that acquisition alignment has been achieved

#### **3.4.2.7 SUS**

commands to align/misalign/scan in angle

### **3.4.2.8 SEI**

none

## **3.4.3. Optical Interfaces**

### **3.4.3.1 Vacuum Equipment**

Movable targets, perhaps in the form of iris diaphragms, will be used to center the beam. The position of these targets will be related to monuments whose position is determined using GPS. The targets are in the ASC, but will require connection to the VacEq, and feedthroughs for control signals.

### **3.4.3.2 SUS**

possible physical interface to coarse alignment sensors

### **3.4.3.3 SEI**

possible physical interface to coarse alignment sensors

### **3.4.3.4 CDS**

TBD.

## **3.4.4. Mechanical interfaces**

### **3.4.4.1 Facilities**

Monuments for the initial alignment fiducials will be required.

space around the fiducials will be needed to allow sighting, adjustments, etc.

### **3.4.4.2 Vacuum Equipment**

Movable targets, perhaps in the form of iris diaphragms, will be used to center the beam. The position of these targets will be related to monuments whose position is determined using GPS. The targets are in the ASC, but will require connection to the VacEq, and feedthroughs for control signals.

## **3.4.5. Electrical interfaces**

### **3.4.5.1 Vacuum Equipment**

Movable targets, perhaps in the form of iris diaphragms, will be used to center the beam. The position of these targets will be related to monuments whose position is determined using GPS. The targets are in the ASC, but will require connection to the VacEq, and feedthroughs for control signals.

## **3.4.6. Diagnostic interfaces**

TBD.

## **3.4.7. Data collection interfaces**

TBD.

## 3.5. Physical and Environmental requirements

TBD.

## 3.6. Test Plan

TBD.

# 4 OPTICAL LEVER SUBSYSTEM

## 4.1. Scope and Objectives

The Optical lever system maintains a predetermined angle of a suspended optic for an intermediate duration. It is the primary control system once the initial alignment has brought the optics to within the range of the Optical Lever, and until the Wavefront sensing system starts to function. It has a stability and a noise performance which allows operation of the interferometers at their design sensitivity for short times (order of 10 minutes) to allow diagnostic tests.

No fabrication of final (deliverable) Optlevs is presently planned in the ASC task; the design will be handed off to the Core optics and I/O optics tasks, and manufacture, test, and final integration of the Optlevs will be performed by those subsystems teams. The pointing and noise performance requirements of the Optlev design may be different for the Mode Cleaner and the Main Interferometer optics. Designs for both will be produced.

The optical path inside the vacuum equipment is also part of this task, and stay-clear zones will be determined for passage of the beam.

## 4.2. Conceptual Design

The Optical lever (Optlev) uses an optical lever to produce a position change on a quadrant photodetector (quaddiode) due to angular motion of a suspended component. The resulting signal is used as an 'error signal' in a servo loop to apply corrective forces to the mirror (via the suspended component actuators, presently magnets and coils). See Figure 4 on page 21 for a sketch. The Optlev consists of a collimated laser source and active beam steering system, a position sensitive monitor of the light transmitted through the suspended optic (the reference quaddiode), and a position sensitive detector of the reflected light (the measurement quaddiode). All three components are mounted on monuments (in task) and to the floor of the facility. An alternative to reduce sensitivity to foundation slab distortion is to mount the laser and the measurement diodes on a low-thermal-expansion optical table somewhat decoupled from the slab. A conceptual layout of Optical Levers has been made<sup>1</sup> for the purposes of testing the Vacuum Equipment conceptual design for flexibility; this is for reference only, but shows the basic feasibility of the baseline Optical Lever approach. The vacuum viewports are also part of the task.

The Optlev serves to reduce the angular motion of the test mass to operational levels. The excitation comes from seismic motion as transmitted by the seismic isolation system and suspension system; resonances, notably that of the suspension system, can bring the level of motion well above the initial level of excitation. The closed-loop Optlev control system actively damps the motion due to the suspension resonance (around 0.5 Hz for the angular motions), thus changing the transfer function of the suspension near the suspension resonances. Stack resonances are not reduced in their  $Q$ , but gain in the Optlev control loop can reduce the net angular motion of the optic due to these resonances.

---

1. Abramovici and Zucker, Vacuum Equipment TIGER Team documentation, March 1993

The reference quadrant photodiode is used in a closed-loop servo system to stabilize the position of the light source as it falls on the suspended optic; this reduces first order sensitivity to beam motion of the Optlev laser beam. A fiber-pigtailed diode laser is used to reduce high-frequency beam jitter and allow rapid replacement of the laser without need for a re-alignment.

A large range mode, using either auxiliary lenses or photodiodes, may be required by the Initial Alignment subsystem (up to planned port sizes).

While in operation, the Wavefront sensor continually updates the null point of the Optlev system such that if the Wavefront system ceases to operate (e.g., loss of longitudinal lock), the Optlev can seamlessly take over control of the optic. Similarly, if a failure of an Optlev unit takes place (e.g., failure of a Optlev laser), the output control signals will be held at their last good value to maintain a nominally correct alignment for a short interim period.

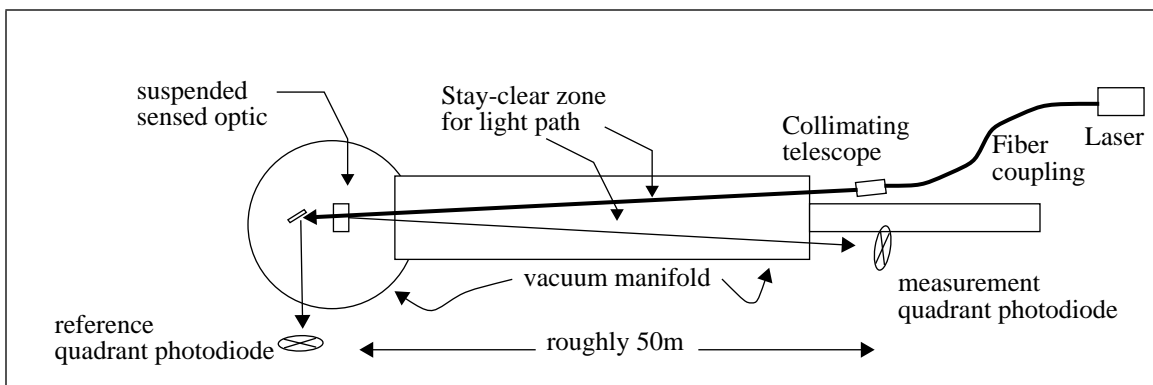


**Figure 4: Conceptual design of an optical lever**

### 4.2.1. Alternatives to the baseline Optical Lever

There are several possibilities for alternative approaches to respond to necessity (insufficient slab stability) or opportunity (availability of quieter and more stable suspension's sensors). Discussions of alternatives to the baseline optical lever are found in an appendix (Section 7.3. on page 37)

## 4.3. Interface Requirements

### 4.3.1. Parameter interfaces: inputs to the Optlev subsystem

**Table 4: Interface Parameters for the Optlev subsystem**

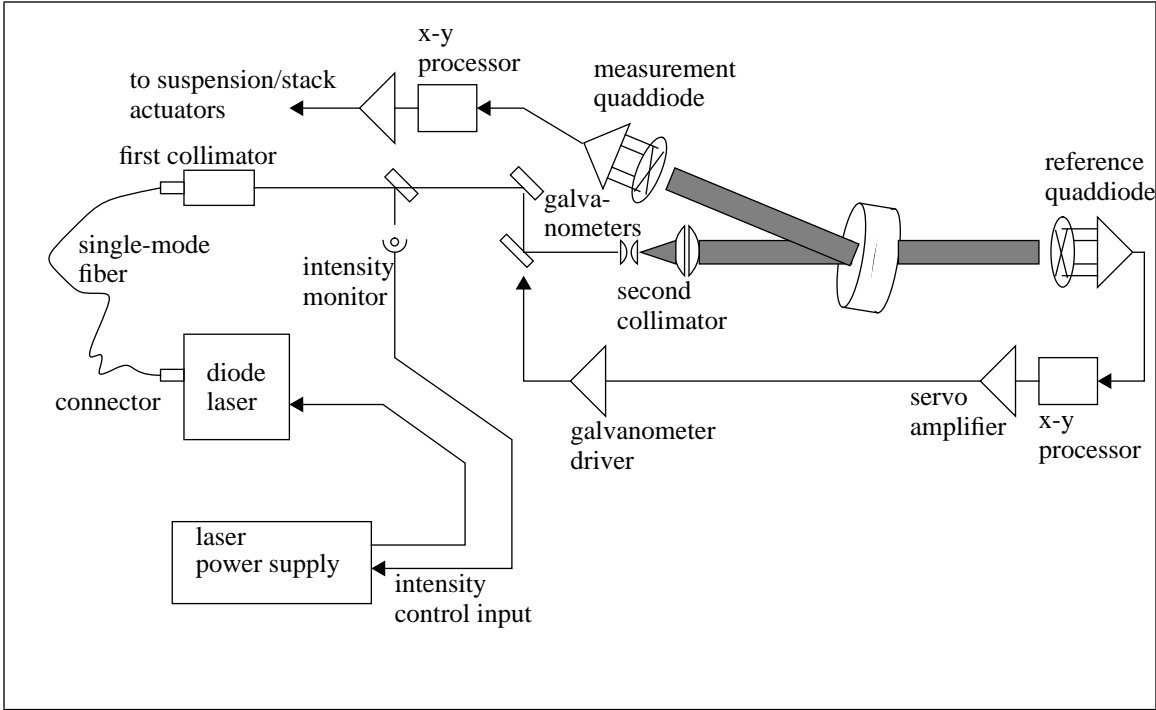


**Figure 5: Functional block diagram of the Optical Lever**

<i>Requirement</i>	<i>Source</i>	<i>Value</i>	<i>Paragraph</i>
slab stability (rms and peak motion, 1 minute, 10 minute, 6 hour times)	FAC	TBD	4.3.1.1
RMS pitch angular seismic, stack drift, stack resonance excitation of optic	SUS	$7 \times 10^{-9}$ rad at 0.5 Hz; $1 \times 10^{-8}$ at 0.1 Hz	4.3.1.2
RMS yaw angular seismic, stack drift, stack resonance excitation of optic	SUS	$7 \times 10^{-9}$ rad at 0.5 Hz; $3 \times 10^{-7}$ at 0.1 Hz	4.3.1.2
lifetime and allowed repair time	SYS	TBD; order of 1 year, order of 1 hour	4.3.1.3
restrictions on wavelength and power of Optlev laser	SYS	TBD; 1 to 0.5 $\mu$ ; order of 10 mW	4.3.1.4

**4.3.1.1 FAC: slab stability (rms and peak motion, 1 minute, 10 minute, 6 hour times)**

See 2.4.1.11, pg. 10 for a discussion.

**4.3.1.2 SUS: RMS pitch and yaw angular excitation of optic**

The excitation due to seismic excitation, stack drift, or resonances in the stack excited by seismic noise must be suppressed to meet the alignment requirement during operation by the Optical Lever system. Since the levels for most of the degrees of freedom and time scales are within the alignment tolerance of the interferometer, the requirement to supply damping to the mass determines the servoloop gain distribution.

### 4.3.1.3 **SYS: lifetime and allowed repair time**

There will be roughly 15 Optlevs per interferometer. Diode lasers have limited lifetimes; the other components of the Optlevs have much longer lifetimes (although are susceptible to damage, from e.g., excess light intensity from the main GW-sensing laser). Failure of an Optlev would usually make the interferometer inoperational, and so the lifetime and the replacement time for the diode lasers (in particular) must be specified carefully. With connectorized fibers, the replacement will be quick and easy.

### 4.3.1.4 **SYS: restrictions on wavelength and power of Optlev laser**

The wavelength restrictions come from the transparency of the viewport and optical components, the coating reflectivity of the optics designed for the GW-sensing laser wavelength, and possibly a requirement that the beam be visible (not infrared) for ease of initial alignment. The power will be limited to a level which will not harm photodiodes under foreseeable circumstances. The beam need not be eye-safe.

## 4.3.2. **Parameter interfaces: demands made by the Optlev system**

These are indicated in Table 3, "Requirement demands placed by the ASC on other systems," on page 12.

## 4.3.3. **Optical interfaces**

### 4.3.3.1 **stay-clear zones**

The Optical Lever beams use some of the beam tube for the Optlev sensing beams. In some cases, other subsystems (especially Suspension and Core Optics) will have priority to establish unavailable paths; in other cases, Optlev will place requirements on other subsystems (Suspension, Core/Support Optics, I/O Optics, Vacuum Equipment) to leave certain zones free. The zones in question are

- light path from optlev laser to sensed optic
- light path from optic to reference quaddiode
- light path from optic to measurement quaddiode
- folding mirror placement behind (and possibly in front) of suspended optics

## 4.3.4. **Mechanical interfaces**

### 4.3.4.1 **monuments:**

- Optlev laser
- reference quaddiode
- measurement quaddiode

### 4.3.4.2 **viewports:**

Nominal 20cm tube necks; 6" or 7.5" (quartz; expensive) viewports possible. Plan on 6" = 15cm

- optlev input laser beam (diameter, transparency at Optlev wavelength)
- reference beam (diameter, transparency at Optlev wavelength)
- measurement quaddiode (diameter, transparency at Optlev wavelength)

### 4.3.4.3 **tables and extra-vacuum clearance**

- for Wavefront sensors per se

- to share with LSC
- adequate physical alignment space around tables

#### 4.3.4.4 in-vacuum components:

- possible steering mirrors

### 4.3.5. Electrical interfaces

This category is designed to cover signals (information) carried by electrical or fiber optics, but not information carried by the GW-sensing beam. To include the subcategories of

- controls
- diagnostics
- data collection

#### 4.3.5.1 signals to the optics suspension control systems (angular information)

- altitude
- attitude
- Optlev in/out of operation (if out, OSEMS must control optic)

#### 4.3.5.2 signals from the Wavefront sensing subsystem

- update to error signal of correct alignment (angular information)
- Wavefront subsystem in/out of operation (if out, Optlev must control optic)

#### 4.3.5.3 CDS backbone:

- state instructions and readout
- power

### 4.3.6. Diagnostic interfaces

TBD.

### 4.3.7. Data collection interfaces

TBD.

## 4.4. Functional and Performance specifications

**Table 5: Physical and Environmental specifications for the Optlev subsystem**

<i>Requirement</i>	<i>Source</i>	<i>Value</i>	<i>Paragraph</i>
noise performance of Optlev	ASC	$1 \times 10^{-8}$ rad	4.4.1.
range of Optlev	ASC	TBR; order of 3 mrad (Optlev align.); $2 \times 10^{-4}$ rad (operational)	4.4.2.



<i>Requirement</i>	<i>Source</i>	<i>Value</i>	<i>Paragraph</i>
power of Optlev laser	ASC	0.1 mW	4.4.3.
frequency stability of Optlev laser	ASC	TBD	4.4.4.
wavelength of Optlev laser	ASC	400nm - 800 nm	4.4.5.
Optlev laser 1/f intensity noise	ASC	$dI/I < 2 \times 10^{-4}$ from 0.1 to 10 Hz	4.4.6.
Optlev beam sizes	ASC	$w_0 \approx 3 \pm 1$ mm.	4.4.7.
quaddiode and amplifier performance	ASC	TBD	4.4.8.
Optlev intrinsic long-term laser beam stability	ASC	$< 1 \times 10^{-4}$ rad for 100 secs	4.4.9.
Optlev pointing servo system performance	ASC	TBD; $1 \times 10^{-8}$ rad	4.4.10.

#### 4.4.1. ASC System: noise performance of Optlev

The optical lever sensing noise must be less than the alignment precision called out in Section 2.2.1., “Principal Interferometer optics angular alignment tolerance,” on page 2; a suitable safety factor must be used. A safety factor of 3 is used.

In addition, the Optlev signal must not contribute noise above the overall interferometer envelope in the GW band; this is addressed in Section 4.4.3.

#### 4.4.2. ASC System: range of Optlev

The range is required to be sufficient to transfer from the suspension’s sensors during the initial alignment and to maintain Optlev linear operation for a practical acquisition time. There are trade-offs of Optical lever length, viewport diameter, and Optlev detector size.

Two different ranges are cited.

##### 4.4.2.1 high sensitivity (operational capability)

for the initial alignment of the Optical lever, the Viewport is a practical limit to the range of output beams that can be sensed. For  $l = 50$  m long arm, and a Viewport clear aperture of 15 cm, the maximum range of angles possible is 3 mrad. This is a workable value, and so is adopted as a specification.

##### 4.4.2.2 large range (search and recovery)

For operation of the Optical lever, the size of available diodes gives a practical limit. For a 50 m long arm, and a quaddiode diameter of 1 cm, the maximum range of angles possible is  $2 \times 10^{-4}$  rad. This is a workable value, and so is adopted as a specification.

#### 4.4.3. power of Optlev laser

There are constraints from the low-frequency control regime, and from the high-frequency GW band.

##### 4.4.3.1 control frequencies (10 Hz-0.001 Hz)

- Shot Noise: For a  $l=50\text{m}$  arm and a  $d=3\text{mm}$  diameter beam, the rate of change of intensity  $I$  for a total intensity of  $I_0$  with position  $x$  is approximately  $dI/dx \approx I_0/d$  and the shot noise is  $i = \sqrt{2eI}\text{amp}/\sqrt{\text{Hz}}$ . The resulting position noise is  $x = d\sqrt{2(e/I)}$  (to within factors of 2). With a typical quaddiode efficiency of  $\eta=1/4$  amp/watt, we find that to meet our requirement of  $\theta = 10^{-8}$  rad with a bandwidth of  $BW=0.1$  to  $10$  Hz, we need

$$P = \frac{1}{\eta} \frac{2ed^2}{(I\theta)^2 BW} = 4 \times \frac{2(1.6 \times 10^{-19})(3 \times 10^{-3})^2}{(50 \times 1 \times 10^{-8})^2 \times 10.1} = 5 \times 10^{-12} \text{W} \quad (\text{EQ 2})$$

- Photodetector/amplifier noise: At the low frequencies of intended operation, a typical current amplifier for this application would have  $10 \text{ pA}/\sqrt{\text{Hz}}$ ; this corresponds to  $1.2 \times 10^{-10} \text{ W}$  of needed power for the signal to be comparable to this noise source; this places a stronger requirement than does the shot noise.

#### 4.4.3.2 GW frequencies (10 Hz-3 kHz)

- Beam motion at GW frequencies must be such that the product of (the signal from this motion) and (the forward transfer function from the quaddiode to the suspensions's actuator) cause angular motions of the mass which have a negligible effect on the GW sensitivity. The simplest way to guarantee this is to require that the motions be smaller than the angular seismic noise. Using the DHS RMS Noise memo as a reference, the angular motion (in attitude) of the mass at  $70 \text{ Hz}$  is roughly  $5 \times 10^{-19} \text{ rad}/\sqrt{\text{Hz}}$ . The forward gain will be of the order of  $2 \times 10^{-9}$  for roughly unity gain at  $1 \text{ Hz}$  (damping, from S/ Kawamura's suspension calculations). This dictates a sensing noise of  $2.5 \times 10^{-10} \text{ rad}/\sqrt{\text{Hz}}$ , or a light power of  $8 \times 10^{-8} \text{ W}$ . TBD; this must be calculated more carefully.
- Ease of alignment (finding the beam with the eye or CCD camera, etc.) leads to a greater power requirement of roughly  $0.1 \text{ mW}$ . This is in the range of commercially available products at a variety of wavelengths with reasonable lifetimes.

#### 4.4.4. frequency stability of Optlev laser

Frequency fluctuations in the Optlev laser can lead to excess noise due to parasitic interferometers. To limit this, the Optlev laser must be single longitudinal mode and have a temperature controller to maintain operation without mode hops. If necessary, a monitor to temporarily (for an msec or so) suspend closed loop control during a rare mode hop will be developed.

#### 4.4.5. wavelength of Optlev laser

The wavelength has only weak constraints.

- We require that the wavelength be visible with the human eye. This is an aid in alignment and debugging.
- The transmission through the designed coatings for the GW-sensing laser should be not less than 0.1 and not greater than 0.9 (to allow both beams to be used)
- The availability of laser diodes adds more wavelength constraints.

We specify that the wavelength be between  $400 \text{ nm}$  and  $800 \text{ nm}$ , TBR.

#### 4.4.6. Optlev laser 1/f intensity noise

Variations in the intensity of the Optlev laser can mimic motions of the beam, and thus constitutes a competing noise source. Using formulæ and values above, we see that  $dI/I = dx/d = (l/d)d\theta$  or that a fractional intensity noise of  $dI/I < 2 \times 10^{-4}$  would be just equivalent to our required sensitivity. This noise is suppressed by normalizing the difference of quaddiode elements (left/right or top/bottom) to the total current, and thus is reduced in its coupling by a factor which is of the order of 10. Including a safety factor of 10 gives a requirement of  $dI/I < 2 \times 10^{-4}$  over the

bandwidth from 0.1 to 10 Hz. This may require some active stabilization, using the sum signal discussed above.

#### 4.4.7. Optlev beam sizes

Constraints on the beams sizes come from the

- viewport diameter (15 cm free aperture)
- stay-free zones (desire to minimize beam diameter, with roughly 10 mm the point of diminishing returns)
- collimator design (less expensive to use smaller optics)
- quaddiode sizes (integrated quadrant photodiodes are available up to 1.5 cm diameter)
- sensing sensitivity (smaller spots make larger  $dI/d\theta$ )
- diffraction limit for the length and distance traveled. For a beam which grows by  $\sqrt{2}$  from waist to maximum over the nominal distance and with a nominal wavelength, this leads to  $w_0 \approx 3$  mm, or a maximum  $1/e^2$  diameter of 12 mm.

The beam is thus specified to have a  $w_0 \approx 3 \pm 1$  mm.

#### 4.4.8. quaddiode and amplifier

Top-level specifications for the photodiode and for the amplifier performance are given here.

quaddiode size (TBD, about 1.5 cm diameter)

quaddiode quadrant separation (TBD;  $<1/100$  quadrant size)

quaddiode maximum current (TBD; 10 mW)

amplifiers (TBD; gain, bandwidth, noise, range)

#### 4.4.9. Optlev intrinsic long-term laser beam stability

The laser beam from the collimator must be sufficiently stable in position (before any active control) to align the beam and place it on the reference quaddiode. This leads to a requirement of beam wander integrated for 100 secs of less than an angle corresponding to the quaddiode radius (order of 5 mm) viewed from a distance of the Optical lever baseline (order of 50 m), or  $<1 \times 10^{-4}$  rad for 100 secs. This drift could be due to either thermal distortions of the collimator or motions of the Optlev collimator support.

#### 4.4.10. Optlev pointing servo system performance

There is an active stabilization of the Optlev beam position where the reference diode signal is the servo error signal held to a minimum, and mirrors mounted on electromagnetic galvanometers are the actuators. The bandwidth of the servo system will be limited by the mechanical characteristics of the galvanometer actuators. The performance requirement is that the integrated residual angle motion of the Optlev beam be less than  $1 \times 10^{-8}$  rad over time periods up to TBR 100 secs. If the primary source of Optlev beam jitter is the LIGO translational seismic noise acting over a baseline of 1m (a worst-case scenario for the angular seismic noise), then the integrated input spectrum is of the order of  $4 \times 10^{-7}$  rad (ref DHS RMS), with most of the contribution coming from the 0.1-0.3 Hz region. Foundation slab distortions and resonances, collimator acoustic excitation, and unshielded air paths are some of the additional input noise with which this servo system must deal. Using the seismic estimate above, a unity-gain frequency of some 20 Hz will be sufficient and easily achievable.

The signal-to-noise issues for the primary Optlev sensing apply here; see Section 4.4.1., “ASC System: noise performance of Optlev,” on page 24.

A more detailed study will lead to specifications for:

- servo gain as a function of frequency
- galvanometer first resonance, torque
- dynamic range
- gain required to deal with stack resonances
- gain required to deal with microseismic peak (in attitude; altitude no problem)

## 4.5. Physical and Environmental specifications for the Optlev

### 4.6. Test Plan

A prototype will be built and tested to meet the requirements. The units to be installed will be tested by the subsystem (IOO Input/Output Optics, COC Core Optics Components). ASC will develop the testing procedure. The system can be broken into the Optlev laser and its beam pointing stabilization on the one hand, and the quaddiode sensors and processing electronics on the other hand; refer to Figure 5, “Functional block diagram of the Optical Lever,” on page 21.

#### 4.6.1. Test of Optlev laser assembly

The laser, power supply, fiber, and collimator are tested to see that they meet specifications:

- The intensity control input is exercised to see that it will respond correctly to the intensity monitor signal.
- The output beam is analyzed (Spiricon or equiv.) to determine if the beam characteristics and quality are acceptable.
- The laser power and intensity stability (calibrated photodiode) and frequency (scanning FP) are measured with the fiber and collimator removed and attached.

#### 4.6.2. Test of Optlev sensors, servo and processing electronics

To facilitate these tests, a reference Optlev and sensors is set up on a testbed with a short baseline. Its functioning is periodically tested.

- The intensity monitor photodiode/amplifier is tested with the reference Optlev laser to ensure proper functioning.
- The galvanometers with their drive are exercised and their range and noise (using the standard sensors) are measured.
- The measurement and reference quaddiodes/amplifiers/x-y processors are each characterized using the standard beam and standard galvanometers to test gain, range, linearity, etc.
- The servo amplifiers for the galvanometers and the suspensions are tested off-line with standard electronics tools.

## 5 WAVEFRONT SENSING SUBSYSTEM

### 5.1. Scope and Objectives

The wavefront sensing system determines the correct alignment of the interferometer by sensing the phase shifts due to a misalignment. It makes no reference to monuments; only the light used for the interferometry is used. The Wave-

front Sensing subsystem includes the sensors, and the processing electronics to produce control signals appropriate for each of the optical elements of the interferometer.

The design of the Wavefront sensing system is planned for FY 96. The cursory description below is only designed to show the basic relationship of this system to the other systems.

## 5.2. Conceptual Design

The basic wavefront sensing mechanism makes use of the RF phase-modulation sidebands applied for the longitudinal sensing system. The wavefront is sensed by multi-segment photodiodes which sample the light at selected points in the interferometer, and each segment is demodulated at the RF phase-modulation frequencies present in the light. Furthermore, a light sample will in general be photodetected at two points in the evolution of the Guoy phase (for example, the near and far fields). The signals from the various photodetectors is combined to form signals which are applied to the actuators determining the interferometer optics angular orientation to bring the sensed ‘error signal’ to zero. The result is a null servo system which optimizes the interference quality without reference to external monuments. The same technique will be used to determine the ‘matching’ of the gaussian beam to the interferometer cavities. No active control of the matching is anticipated, but the information can be used for initial interferometer setup and to monitor degradation in the matching (due, for instance, to mirror heating).

In practice, the multi-segment photodetectors will probably be placed at the same ports as the length photodetectors, or such that ‘wedge beams’ are monitored. The detailed design will follow the design of the length sensing system.

## 5.3. Interface Requirements

### 5.3.1. Parameter interfaces: inputs to the Wavefront Sensing Design

#### 5.3.1.1 ASC System: operational alignment requirement

See Section 2.2.1., “Principal Interferometer optics angular alignment tolerance,” on page 2

#### 5.3.1.2 ASC System: operational seismic and thermal motion of the suspended masses

Section 2.4.1.2, “SYS: seismic and thermal noise limited gravitational-wave sensitivity,” on page 7

#### 5.3.1.3 IOO: matching into GW-sensing interferometer

possible difficulties due to poor matching

#### 5.3.1.4 LSC: length sensing configuration and performance

Section 2.4.1.3, “LSC: length sensing configuration and performance,” on page 7

#### 5.3.1.5 COC: core optics specifications

Section 2.4.1.5, “COC: core optics requirements,” on page 8

#### 5.3.1.6 SYS: operations scenario

Section 2.4.1.13, “SYS: operations scenario,” on page 11; in particular,

- time to relock after short dropout

- design continuous locked time

## 5.3.2. Parameter interfaces: demands made by the Wavefront Sensing Design

### 5.3.2.1 COC: beam samples (wedge beams)

- beams in addition to those required by length. TBD, but this is probably limited to the wedge beams from the two near test masses.
- intensities of wedge beams (thus AR coatings of Core Optics). Needs to give usable noise performance. Order of magnitude of 50 mW (consistent with 1000 ppm reflection)
- uniformity of intensity and phase of wedge beams. Required to make transformation from near to far field using telescopes. Rough estimate is that we do not want more than several percent of the power to be scattered into the  $TEM_{01}$  mode from the  $TEM_{00}$  by whatever lack of uniformity.

### 5.3.2.2 LOS: actuators

- actuators on suspended masses: bandwidth, noise
- actuators on stack support points: resolution, noise, range

## 5.3.3. Optical interfaces

TBD GW-sensing beam ports to be used. Some to be in common with LSC sensing ports, others to be wedge beams. All external to the vacuum.

## 5.3.4. Mechanical interfaces

Tables at the sensed ports, with supports

Room around tables for initial setup, troubleshooting

## 5.3.5. Electrical interfaces

TBD.

## 5.3.6. Diagnostic interfaces

TBD.

## 5.3.7. Data collection interfaces

TBD.

# 5.4. Functional and Performance specifications

## 5.4.1. Wavefront sensor shot-noise-limited sensitivity

TBD.

### 5.4.2. Wavefront sensor electrical range

TBD.

### 5.4.3. Wavefront sensor RF frequency response

TBD.

## 5.5. Physical and Environmental requirements

TBD.

## 5.6. Test plan

TBD.

# 6 CENTERING SUBSYSTEM

## 6.1. Scope and Objectives

The requirements and means for positioning the main laser beam accurately on the surface of the suspended optics are addressed by the Centering system. Translations of the optic perpendicular to the beam (in the horizontal and/or vertical) are needed to bring the optical axis into line with the center of rotation of the optic, and this position must then be maintained. We refer loosely to this as ‘centering the beam’, although it may not be in the geometric center of the optic.

## 6.2. Conceptual design

The basic motivation for establishing a requirement for the positioning of the main beam (here called the ‘GW-sensing beam’ to distinguish it from auxiliary ‘red beams’) on the suspended optics is to limit the coupling of rotational motion of the test mass about its center of mass to length changes along the optical axis.

### 6.2.1. Determining the correct position of the mirror

The approach taken is to make an intentional periodic rotation of the optic to be centered on the beam and to analyze the interferometer output to minimize the observed coupling. This procedure is performed at intervals as needed, but not more often than once per day; the procedure is automated to make the total duration acceptable with respect to the operations scenario.

In somewhat more detail, an automated procedure applies a sinusoidal excitation at a frequency within the normal GW band (order of 100 Hz) to one of the angular degrees of freedom of the optic in question. The output of the interferometer is synchronously demodulated at the modulation frequency, and the resulting signal is proportional to the difference from the correct beam positioning and carries a sign which indicates the correct relative motion between the beam and the optic to bring the signal to zero. The needed translations of the optic or the beam (depending on the optic) are made, and the new position is stored for reference.

## 6.2.2. Maintaining the correct position

The facility is sufficiently stable such that the periodic determination of the correct position can be made rarely enough to not disturb operation of the interferometer, and no additional sensing or maintenance need be pursued. The facility slab due to thermal changes which would allow for daily, or less frequent, centering measurement and correction.

Other sources of drift in position are the seismic isolation stack, barometric pressure changes leading to forces on the slab from the Vacuum Equipment, and mechanical stress release in the suspension.

## 6.2.3. Actuators

In general, a combination of actuators will be used to correct a given positioning error, and an intelligent controller will be needed to correctly develop the right response to a given set of perceived centering errors.

- laser beam position: The laser beam position in the straight-through arm (beamsplitter transmitted beam) will be determined by steering mirrors after the mode cleaner. This will be the preferred actuator for at least the far mirror on this arm, and sometimes the near mirror as well. The beamsplitter angle will do the same for the other (beamsplitter reflected beam) arm.
- stack drift compensators: This will be the only way to make vertical translations of the optic (of course, when possible, the GW-sensing beam can be translated in the vertical). Compensators can also be used to take out long-term horizontal drift. See Section 2.4.2.3 on page 13.

## 6.3. Interface Requirements

### 6.3.1. Parameter interfaces: inputs to the Centering Design

slab distortions leading to tilts which then lead to mirror displacements (w.r.t. sensors, like beam pointing sensor, behind mirror)

### 6.3.2. Parameter interfaces: demands made by the Centering Sensing Design

#### 6.3.2.1 LOS: actuators

- actuators on suspended masses: bandwidth, noise
- actuators on stack support points: resolution, noise, range

### 6.3.3. Optical interfaces

TBD.

### 6.3.4. Mechanical interfaces

TBD.

### 6.3.5. Electrical interfaces

TBD.



### 6.3.6. Diagnostic interfaces

TBD.

### 6.3.7. Data collection interfaces

TBD.

## 6.4. Functional and Performance specifications

### 6.4.1. Sources of drift

#### 6.4.1.1 stack drift, ground tilts

Drift is motion slow compared to the pendulum suspension resonant frequencies, so times of the order of several seconds and longer. There will be differential changes in the stack height due to temperature changes and inelastic flow; there will be shifts in the support structure due to atmospheric pressure changes and temperature changes; there will be drifts in the floor angle due to lunar tidal forces. Need to check stack documents (Sievers and Shoemaker for the first and second VacEq tiger teams), but this is of the order of tens to hundreds of microns. These angular drifts can induce translations of the optic with respect to the beam via the lever arm of the height of the stack tower, several meters.

#### 6.4.1.2 laser beam pointing

The pointing of the initial GW-sensing beam will also drift with angular drifts of the launching optics, but now with the lever arm of the 4km arm. The centering sensors will be, in fact, the primary reference for the long-term stability of the GW-sensing beam pointing.

#### 6.4.1.3 vertical wire stretching

Some drift is anticipated from the vertical stretching of the suspension wire.

### 6.4.2. Relationship to other control systems

Coupling from one control system to another can either lead to servo complications or instabilities, or noise coupling. Given the low unity-gain of the centering system (roughly 0.1 to 1 Hz), we would expect the servo problems at these low frequencies. Noise coupling is most likely to be a problem at GW frequencies (50 Hz and up).

The length, centering, and angular control systems are ideally orthogonal. In fact, the sensors and actuators both can lead to cross-terms. The most likely source of cross-terms is poor balancing of the four magnet-coil drivers in the suspension system or poor alignment of the sideways driver magnet(s). (A pair of magnets and coils on the two sides of the mirror could be used to largely null this effect.) Both the low frequency (close to the suspension resonant frequencies, <10 Hz) and ‘AC’ (GW frequencies, >50 Hz) balancing are important to characterize servo stability and noise cross-coupling.

#### 6.4.2.1 length control

One type of coupling is just the effect which we wish to minimize with the centering control system, that is, a change in length of an interferometer arm due to a rotation of the test mass. This is discussed in the requirements section above, and is the one coupling mechanism likely to be important.

Another possible coupling is due to actuators not acting exactly along the desired axis. If the length control system, which should only exert forces along the optic axis, has a coefficient along either the vertical or horizontal transverse axis, an unintentional translation will take place.

#### **6.4.2.2 pointing**

Coupling could take place between the local angular control system (pointing system) and the centering system: If in making an angular change, some translational force were accidentally applied, the optic would translate in response to a desired angle change.

Alternatively, if the translation actuators also cause an accidental rotation or tilt of the mirror, a cross-coupling term will exist.

#### **6.4.2.3 phase front sensing**

A translation of a curved mirror will lead to a change in the optical axis of the cavity and thus to a misalignment. This will be sensed by the alignment system and corrected. This is a coupling between the two systems.

A change in the beam pointing (as requested by, for example, a far mirror centering system) will probably be made by a simple angle change in the beam injected into the cavity. This introduces a misalignment of the cavity, and the mirrors must be rotated to correct for this. The alignment system will correctly sense this. It is, however, a first order coupling of the two systems.

The alignment must be maintained to about  $3 \times 10^{-8}$  rad rms per mirror, which corresponds to approximately 0.1 mm of motion on a mirror. This is an argument for very different bandwidths for the alignment and centering systems.

### **6.5. Physical and Environmental requirements**

TBD.

### **6.6. Test plan**

TBD.

## 7 APPENDICES

### 7.1. Angular alignment requirement

#### 7.1.1. Basis of the Mode Decomposition Approach

The transverse distribution of an arbitrary paraxial electric field can be expanded as a sum of Hermite-Gaussian modes  $\Psi_{i,j}(x, y)$  and expressed as a vector of the expansion coefficients. In a cavity with slightly tilted mirrors, all but the first three modes  $TEM_{00}$ ,  $TEM_{01}$ ,  $TEM_{10}$  may be dropped since their excitation is negligible. The field vector reflected by a tilted mirror is related to the incident field by a tensor transformation  $M$  which couples light from the  $TEM_{00}$  mode into the  $TEM_{01}$  and/or  $TEM_{10}$ . Free space propagation is given by a tensor  $P$ , where the advance in the Guoy phase  $\text{atan}(z/z_0)$  gives critical information about the beam.

The steady state of the field inside and the field reflected from a Fabry-Perot cavity can be found by solving the matrix equations which describe the arrangement. To solve a compound cavity configuration, one treats the arm cavities first, replacing them with the equivalent matrices  $M$ . The recycled Michelson equation is then solved in a recursive way.

#### 7.1.2. Sensitivity of the LIGO Interferometer to Misalignments

A mathematical model of the proposed LIGO configuration using a symbolic language (Mathematica) has been constructed<sup>1</sup>. The model includes the length sensing system planned for LIGO, in which RF phase modulation at multiple frequencies is applied to the light before it enters the interferometer. Using this model, we calculate the field on the detector at each modulation frequency, and thus the sensitivity to gravitational waves, as well as the detector shot noise.

The sensitivity to gravitational waves is quadratic around the optimum alignment, and can be characterized by the misalignment which reduces the sensitivity to a prescribed value when compared to the perfectly aligned case. The present working value for the allowed derating is 0.9 of the perfectly aligned GW sensitivity. For example, for the recycling mirror, this corresponds to a maximum misalignment of  $\theta_{\text{rec}} = \pm 0.91 \times 10^{-7}$  rad. This quadratic sensitivity for each element leads to a requirement for the sum of the squares of the misalignments of the individual optical elements, weighted by their differing effects on the GW sensitivity; for our baseline 0.9 derating, the requirement becomes

$$\sum_{i=1}^{10} \left( \frac{\theta_i}{\beta_i} \right)^2 < 1 \text{ for } \frac{SNR(\theta_1, \theta_2, \dots)}{SNR(\theta_i=0)} < 0.9 \quad (\text{EQ 3})$$

where  $\beta_i$  are the sensitivities to each of the alignment degrees of freedom. For the LIGO interferometer, the  $\beta_i$  vary between  $9.1 \times 10^{-8}$  and  $2.9 \times 10^{-8}$  radians. Assuming that the mechanical excitation of all the mirrors is similar and that our ability to measure and control their angular motion is the same for all, this error in alignment can be spread over the ten degrees of freedom. For the requirement on the facilities and in general when the factor of three difference between different mirrors can be neglected, we choose the tightest alignment tolerance as being representative. This leads to a requirement of  $3 \times 10^{-8}$  radians rms alignment tolerance. Furthermore, a safety factor should be applied, TBD by the System Integration. We use a baseline safety factor of 3, leading to a requirement of  $1 \times 10^{-8}$  radians rms.

---

1. Hefetz and Mavalvala, in preparation

## 7.2. Centering requirement

The performance specification is developed using the Kawamura-Zucker<sup>1</sup> model for the coupling from a combination of offset from center and GW-band rotational motion to length changes. Note that the centering must be maintained within prescribed limits for both static positioning and dynamic ‘beam wander’ or optic motion.

The optic rotational noise may be due to the angular control system or the filtered seismic noise. We assume in the following that the seismic noise dominates (this puts a requirement on the angular control system noise, to be checked)

There may be other reasons why the interferometer performance will be a function of the position of the beam on the mass, but we use only the above mechanism to determine the system requirements. It is assumed that one of the troubleshooting tools we will need is the ability to translate the test mass with respect to the GW-sensing beam and to monitor this motion and to reproduce a given position with the needed precision, and the centering system automatically gives us this monitor.

We use the paper cited above to develop the specifications for the required centering, and thus the performance requirement for the centering system.

We require that the LIGO sensitivity not be compromised by this noise mechanism. The noise contribution from centering error falls very rapidly with frequency (like the seismic noise), and tracks with the seismic noise---improvements in the seismic isolation for motion along the optical axis reduces proportionately the noise contribution from centering error.

### 7.2.1. Basis of the Centering requirement

We use SK-MZ Eq 15 as our point of departure:

$$S_l(f) \approx [d_1^2 + (2d_1^{rms})^2] S_{\epsilon_1}(f) + [d_2^2 + (2d_2^{rms})^2] S_{\epsilon_2}(f) \quad (\text{EQ 4})$$

$S_l(f)$  is the power spectrum of the length changes in a simple cavity, induced by a combination of length fluctuations in mirror 1 and 2 at GW frequencies (represented by power spectra  $S_{\epsilon_1}(f)$  and  $S_{\epsilon_2}(f)$ ) and static and slowly varying fluctuations in the offset  $[d_1^2 + (2d_1^{rms})^2]$  for mass 1; subscript 2 for mass 2) of the beam spot on the mirror from the point closest to the center of rotation of the mirror. In this nomenclature,  $d_1$  is to be maintained at an acceptably low level by the centering servo system we are discussing here, given the  $d_1^{rms}$  and the  $S_{\epsilon_1}(f)$  which are determined by the performance of the seismic isolation system and mirror control system.

The translational (perpendicular to the beam) rms motion for LIGO can be predicted using the LIGO standard spectrum and the sideways damping from the suspension’s sensor. The LIGO standard ground noise is  $x(f) = 1 \times 10^{-9} \text{ m}/\sqrt{\text{Hz}}$  at 1 Hz; the rms motion resulting will be roughly the  $\sqrt{Q_{\text{damped}}}$  times this. We may choose a low damping to reduce coupling of noise from the damping sensor to the length readout; even if we choose a  $\sqrt{Q_{\text{damped}}} = 100$ , the rms motion will be  $x_{\text{RMS}} \sim 10^{-8} \text{ m}$  rms. This is negligible. In the vertical direction, the frequency is higher (roughly 14 Hz), and the excitation is smaller; however, no damping is anticipated.

The rotational motion is estimated by assuming that the suspension’s actuators output noise increases the suspended optic’s angular motion above the seismic. If suspension actuators drive the edges of the mirror at four points with random noise, there will be both rotational and translational motion of the mirror. Their ratio can be calculated from the

---

1. S. Kawamura, M. Zucker

ratio of the rotational inertia to the translational inertia; this leads to

$$\frac{\theta}{x} = \frac{r}{\left(\frac{l^2}{3} + \frac{r^2}{4}\right)} = 26.1 \text{ rad/m} \quad (\text{EQ 5})$$

for our mirrors ( $r = 0.125 \text{ m}$ ,  $l = 0.05 \text{ half-length}$ ). Perhaps more useful is the ratio of the edge of the mirror motion due to rotation to that due to translation; this is  $(\theta/x)r = 3.3$ . This indicates that the net (sum) translational motion on the mirror has equal contributions from rotations and translation at about 1/3 of the mirror radius. There are eight degrees of freedom of the mirror, and we assume that the electronic noise from them is all uncorrelated, so that the motion from all mirrors is  $\sqrt{8}$  times larger than that of a single mirror.

No other mechanisms for conversion of translations perpendicular to the optic axis (with or without rotational motion) have been considered in detail. Ripples on the mirrors (given the stringent requirements on the surfaces) do not seem to lead to significant effects. Variations in the reflectivity might also add constraints, but probably not interferometric ones (constancy of calibration, for instance, might be affected).

## 7.3. Optlev Alternative Conceptual Designs

### 7.3.1. Re-entrant Optical Lever

The standard Optical Lever uses a ‘V’ optical path; the laser source is placed to one side of the beam tube, the monitor quaddiode is placed at the apex of the V behind the optic to be sensed, and the measurement quaddiode is placed on the other side of the beam tube.

An alternative is to collapse the ‘V’ so that the laser and the measurement quaddiode are very close, so that the return beam is almost coincident with the input beam; the second arm of the ‘V’ is cut short with a return mirror relatively close to the sensed optic (see Figure X). In addition, the reference beam is not detected at the optic, but is also sent back to the source laser by a mirror at the same distance from the sensed optic as the measurement beam return mirror. As before, a servo system can hold the spot on the reference quaddiode constant, and mirror motions cause changes in the measurement beam position on the quaddiode

There are several advantages to this arrangement.

- No first-order error from translations of the laser-quaddiode emplacement with respect to the sensed optic-return mirror emplacement; similarly, no first-order sensitivity to laser beam translations (or confusion with angle changes)
- Same spot size on both reference and measurement quaddiodes; easier beam collimation, better common-mode rejection of beam geometry changes, intensity fluctuations, simpler engineering
- Fewer optical stay-clear zones along the beam tube
- No significant motion of measurement quaddiode with respect to the laser (being on the same monument), thus lower sensitivity to slab distortions
- Laser and quaddiodes all in same physical location; aids engineering and alignment

Drawbacks:

- Rotations of the sensed optic-return mirror emplacement as a unit give the incorrect signal sign (measurement return beam stays fixed (incorrect), and reference beam rotates correctly). Rotations of just the optic are sensed correctly, however. Does this just offset the advantage of translational independence? Can an additional detector behind the mass be used to correct for this?
- Two mirrors must be placed in the vacuum system and aligned (possibly true for the baseline Optical Lever as

well)

## 7.3.2. 4km Optical levers

One of the limitations of the Optical Levers is that the local and slab-to-slab mechanical stability limits the duration of time over which the Optical Lever can maintain operational alignment. Using the full length of the 4km beam tubes for the Optical Levers would in principal allow long-term operation with the Optical Lever; this allows more flexibility in operation, and offers a fall-back position if Wavefront Sensing is not ready for the initial installation. The local and slab-to-slab motions become unimportant, lessening demands on the facility.

### 7.3.2.1 Simple extension of Optlevs to 4km

Several drawbacks are clear. The ‘red’ beams would be the size of the GW-sensing beams (perhaps a bit larger due to a longer wavelength of light), although the clearance required would be less (not necessary to require clearance so far in the wings of the beam). The optics and viewports would be large, or telescopes in vacuum would be required. Much of the beam tube would be filled with the initial interferometer beams (GW-sensing and several red). While it is relatively easy to find a conceptual design for the pointing beams for the main test masses, the beamsplitter and recycling mirror also require pointing of the same precision. Either paths for the large-diameter red beams around the test mass would need to be found, or some alternative means of linking the alignment of the beamsplitter and recycling cavity to the near mirrors would be required. In this alternative, a reference mirror would be aligned using the 4km red beam Optical Levers, and then the other optics (test mass, beamsplitter, recycling mirror) would all be held fixed in alignment (for example, with short optical levers) with respect to this reference mass. A straightforward extension of the baseline design to 4km lengths appears to be impractical. This approach will not be pursued.

### 7.3.2.2 Pulsed Optlev laser approach

Another approach to the 4 km lever arm is to use just one optical lever laser which is directly on the GW-sensing beam axis. It sends out short pulses (order of 1 nsec wide, kHz repetition rate) which propagate down the beam line. Each reflective surface encountered sends back the pulse which is received at a unique time by a quaddiode. By interpreting the series of pulses correctly, information on the alignment of several optics can be obtained with a single beam.

In practice, a pulsed laser diode is used as the light source, and one is placed beyond each 4 km arm end mirror. The measurement quaddiode picks off the return light using a polarization technique resembling the reflection lock of a simple cavity. The quaddiode is gated to select only the main return pulse from a given optic, suppressing multiple bounces and scattered light. A reference quaddiode for each arm is placed at the vertex and is used to stabilize the orientation of the input laser light.

Not all optics return a beam: the beamsplitter and (for the mid-length interferometer) the folding mirror do not directly return a signature pulse. For the beamsplitter, differences of the signals from arm 1 and arm 2 can be taken to separate the angle of the beamsplitter from that of the recycling mirror. No satisfying scheme for reading out the angle of the folding mirror has been developed.

The dynamic range of the system is limited as for the other long optical levers, so the approach is only useful to maintain an alignment which is close to acquisition alignment. Some large optics are needed to collimate the outgoing beam, but the use of gating to suppress undesired light relaxes the beam quality requirements seen for the naive 4km optical lever.

The pulsed aspect of the system has some complications. The development of the driver and receiver circuits would take time and care; electromagnetic interference from the pulses to the GW-sensing electronics could be a problem.

The test masses receive impulses of momentum from the photons, making  $10^{-21}$  m jumps for each pulse received; this will excite test mass and suspension resonances. Uniformity of the pulses is important to keep the net displacement fluctuation below that of other sources (the masses are displaced by roughly  $10^{-19}$  m by the average reflected laser power of a 0.1mW, so moderate repeatability will suffice).

The approach seems to be the most attractive means to tracking slab-to-slab motion for a number of optics. The implementation problems described above would require time and effort to solve, but no fundamental problems are seen. If slab-to-slab tracking is needed, this approach will be pursued further.

### 7.3.3. Use of the main GW-sensing beam as an Optical Lever

The GW-sensing beam itself could also be used as part of a pointing system. The complexities are that the GW-sensing beam is part of a complicated optical arrangement, and its motion due to a misalignment is more difficult to interpret in terms of an individual mirror misalignment. In addition, the intensity of the beam is a strong function of the resonance state of the interferometer, and this requires a dynamic range adaptation.

A principal problem is with the fact that we specifically want something that makes sense before and through the locking procedure, so we would have to understand what the beam intensity patterns mean in all states of misalignment, and for any combination of partial/complete resonance of any cavities, and for any state of the Michelson, and with a dynamic range of  $4\text{kW}/(2W*0.03*0.03*0.5)=4\times 10^6$  for the arm cavities.

### 7.3.4. LED sensors as alternative to Optical Levers

A different approach to maintaining operational alignment long enough to allow locking of the interferometer is to employ the optical position sensors which are integrated into the mass suspension cage (called ‘OSEMs’ in the 1994 40m design). They differ from the baseline Optical Lever design in the fact that the local reference for position is not a monument mounted on the slab floor, but rather the cage attached to the seismic isolation stack. The advantage of this approach is that it may allow the suppression of the Optical Levers, simplifying the optical layout and reducing the complexity of the initial LIGO.

One limitation is due to the low-frequency noise characteristics of the (present) sensor and the position reference it uses. The noise at 1 Hz of the present baseline suspension’s sensor system (edge detection with a single photodiode) is  $1\times 10^{-9}$  m/ $\sqrt{\text{Hz}}$  at 1 Hz, and  $\sqrt{2}\times 10^{-9}$  m/ $\sqrt{\text{Hz}}$  at 0.3 Hz. The sensors are located at about a 10 cm radius from the center of rotation of the test mass, thus, the corresponding angular noise is  $1\times 10^{-8}$  rad/ $\sqrt{\text{Hz}}$  at 1 Hz for one sensor; there may be a factor 2 improvement with 4 sensors (two left added, two right subtracted, and a quadratic addition of the noise). With a high-pass filtering of the sensor in the servo loop at 0.5 Hz, the 0.3 Hz noise could be reduced in the closed-loop control system at lower frequencies (by eliminating closed loop control below roughly 0.5 Hz using this sensor); the bandwidth of noise integration might be of order 4 Hz, cancelling the multiple detector gain. This leads to roughly  $1\times 10^{-8}$  rad rms angular motion from the optical sensor; this is good enough for acquisition, and would marginally allow operation.

The next limit to sensitivity is the seismic isolation stack drift and amplification of seismic motion. The MIT prototype stack showed an average downward drift of 10  $\mu$  m day. If we assume (worst case) that all of the downward drift also leads to a rotation of one edge of the stack by an equivalent amount (a sort of ‘cork-screw’ motion of the stack top plate) then this corresponds to roughly  $2\times 10^{-9}$  rad/sec. This motion would limit operational alignment to 5 seconds and acquisition alignment to about 1 minute; these durations may be acceptable. If slab stability permits, another possibility is to use an Optical Lever to read out the stack drift angular motion, and to either electronically or mechanically (using drift compensators) correct for the drift, thus potentially extending the run-time using the OSEM-like sensors for local readout. There would be one Optical Lever per stack in this scenario, a negligible improvement over

the baseline. The sensor does also suffer from any drift of the slab, and so can be no better than a traditional 50m optical lever. In fact, as it does not use a reference from the far mass, it may suffer more than a traditional Optical lever from slab distortions; local rotations are not sensed at all, whereas in the traditional two-sensor Optical lever, they are strongly suppressed by the beam-pointing servo.

If the solid-body modes of the stack have a high  $Q$ , the amplification of the seismic motion may lead to excessive motion of the cage holding the suspension sensor. How much motion this imparts to the mirror is a detailed question of the frequency-dependent gain in the servo-loop linking the two, but the upper unity-gain frequency of the servo-loop will be of the order of 1 Hz and not much less at 5 Hz. This can apply a requirement on the stack mode  $Q$ 's.

Lastly, the suspension sensor noise is too high in the GW band (50 Hz and greater) to allow operation with the sensor providing the short-term feedback to the suspended optic orientation (which is the baseline model, using the Optical lever for that short-term feedback). At 100 Hz, typical noise is  $2 \times 10^{-10} \text{ m}/\sqrt{\text{Hz}}$  per suspension detector; if a gain of 1 or 3 is needed at 1 Hz to maintain pointing, and one rolls off the gain as quickly as possible above this (a gain of  $2 \times 10^{-9}$ ), the resulting noise at 70 Hz is  $4 \times 10^{-19} \text{ m}/\sqrt{\text{Hz}}$  per sensor, or  $\sqrt{16} = 4$  greater for an incoherent addition of the noise of four sensors on each of the four test masses, which is greater than the anticipated noise from other sources (notably thermal noise of the pendulum). Thus, this sensor could only be used if the design were changed to make the Wavefront sensor the only pointing system for operation. There is reluctance to follow this path because of the complications in the servo-loops that would come from the optical time constants of the interferometer and possible coupling to the length control.